applied sciences

MDPI

Article

Tectono-Stratigraphic Framework and Hydrocarbon Potential in the Albert Rift, Uganda: Insights from Basin and Petroleum System Modeling

Lauben Twinomujuni [1,2,3], Keyu Liu [1,2,*], Hafiz Ahmed Raza Hassan [1,2], Kun Jia [1,2], Shunyu Wang [1,2], Tonny Sserubiri [4] and Mathias Summer [4]

[1] School of Geosciences, China University of Petroleum, Qingdao 266580, China; twinomujunilauben@gmail.com (L.T.); h.ahmedraza1@yahoo.com (H.A.R.H.); jia_work12@163.com (K.J.); wangshunyu1995@163.com (S.W.)
[2] Laoshan National Laboratory, Qingdao 266071, China
[3] Department of Geology and Petroleum Studies, Makerere University, Kampala P.O. Box 7062, Uganda
[4] Directorate of Petroleum, Entebbe P.O. Box 9, Uganda; tsseru@yahoo.co.uk (T.S.); summermathias5@gmail.com (M.S.)
* Correspondence: liukeyu@upc.edu.cn

Abstract: The Albert Rift in Uganda is a significant geological and petroleum exploration frontier within the East African Rift System. The basin has been comprehensively analyzed thorough the means of literature survey, seismic data analysis, well-log interpretation, and basin and petroleum systems modeling to examine the complex interactions of tectonics, sedimentation, and hydrocarbon generation and expulsion within the rift basin. Our findings reveal a detailed tectonostratigraphic framework with multiple Neogene to Quaternary depositional sequences and structural features influencing hydrocarbon maturation, generation, and expulsion. Key stratigraphic units are identified, highlighting their contributions to a viable petroleum system present within the basin. The Albert Rift is a Neogene petroleum system that is currently generating and expelling hydrocarbons to various potential traps. Mid-Miocene sediments were deposited in a favorable lacustrine environment as a viable source rock, which began generating and expelling hydrocarbons from the Middle to Late Pliocene in the deeper parts of the rift basin, while those deposits in shallower areas have only recently entered the oil window and have yet to start major petroleum generation.

Keywords: tectono-stratigraphic framework; petroleum system; basin modeling; Albert Rift in Uganda

Academic Editors: Arcady Dyskin and Fernando Rocha

Received: 19 December 2024
Revised: 21 February 2025
Accepted: 11 March 2025
Published: 13 March 2025

Citation: Twinomujuni, L.; Liu, K.; Hassan, H.A.R.; Jia, K.; Wang, S.; Sserubiri, T.; Summer, M. Tectono-Stratigraphic Framework and Hydrocarbon Potential in the Albert Rift, Uganda: Insights from Basin and Petroleum System Modeling. *Appl. Sci.* **2025**, *15*, 3130. https://doi.org/10.3390/app15063130

1. Introduction

The Albert Rift represents the northernmost extension of the western branch of the East African Rift System (EARS) [1]. Extending approximately 570 km in length and 45 km in width, it spans from South Sudan in the north to Rwanda in the south, straddling the border between Uganda and the Democratic Republic of the Congo (Figures 1 and 2). This rift comprises half-grabens and grabens with varying symmetry and orientations, interspersed with accommodation zones and a prominently elevated basement horst at its center. Relative to the eastern branch of the EARS, the Albert Rift has experienced comparatively less magmatism. This distinctive geological setting, coupled with the presence of the towering Mt. Rwenzori horst within the rift valley, has drawn significant scientific interest aimed at elucidating continental rifting mechanics.

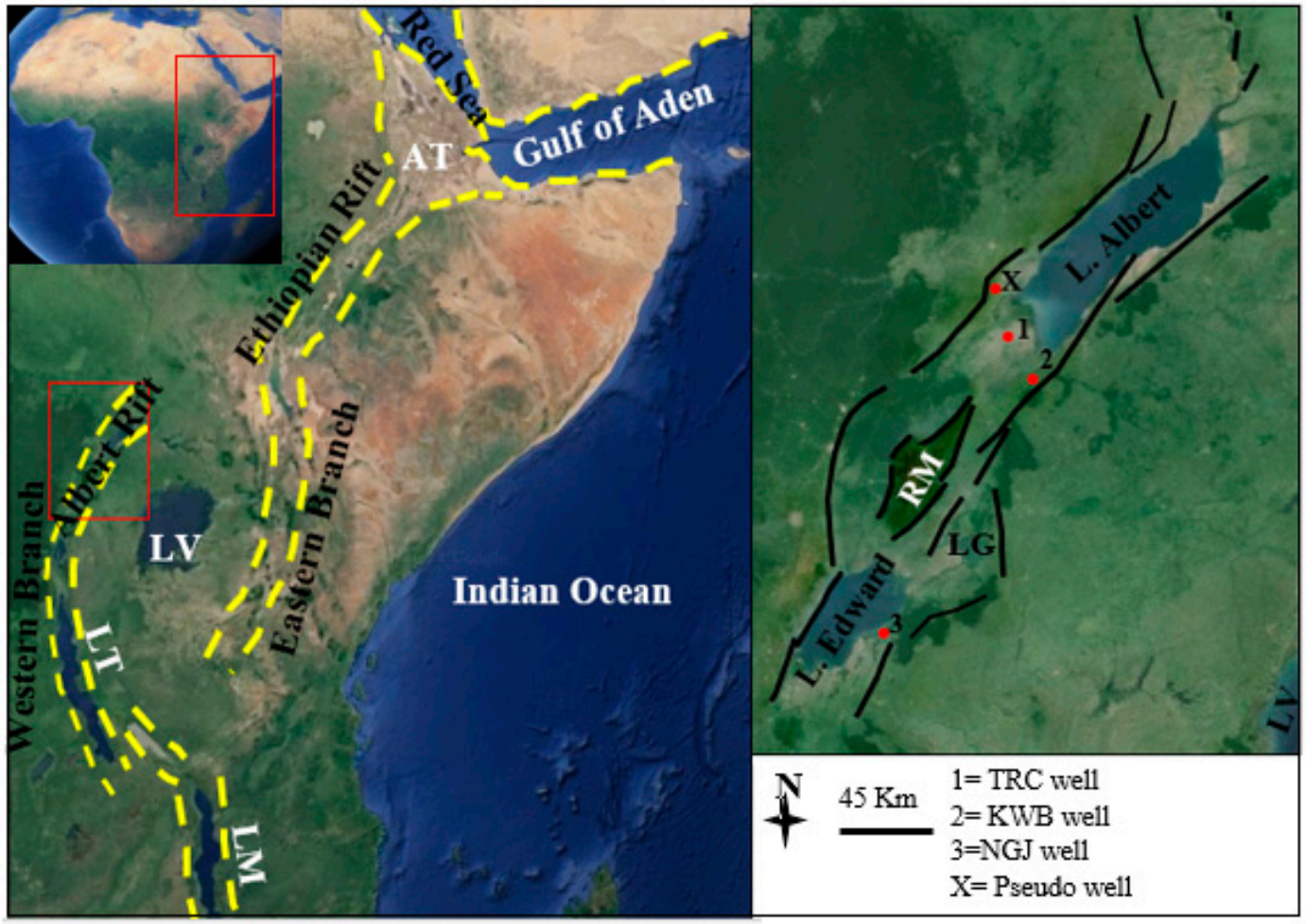

Figure 1. Outline of the Albert Rift in the East African Rift System. EARS = East African Rift System; AT = Afar Triangle; BF = Bunia Fault; NTB = North Toro-Bunyoro Fault; TF = Tonya Fault; KF = Kichwamba Fault; LBF = Lubero Border Fault; RM = Rwenzori Mountains; VM = Virunga Mountain; LV = Lake Victoria; LG = Lake George; LT = Lake Tanganyika; LM = Lake Malawi; DRC = Democratic Republic of the Congo.

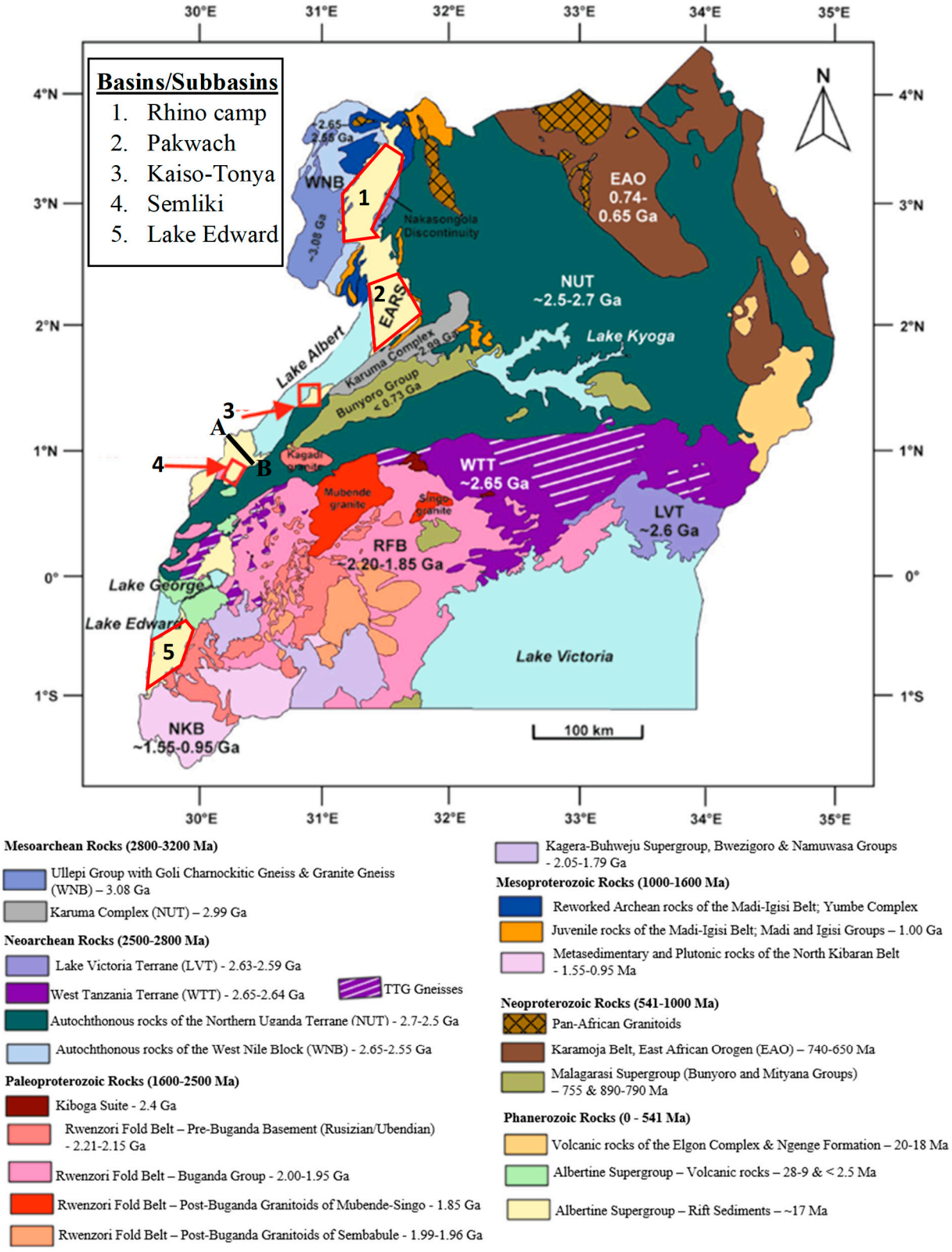

Figure 2. Geology map of Uganda showing the different types of localities where the Albert Rift sediments are well exposed (modified, after Hinderer et al. [2]). The thick black line AB represents the location of the cross-section used for modelling.

The Albert Rift harbors three major lakes—Albert, Edward, and George—which are part of the chain of rift valley lakes in the western branch [3–7]. These lakes have accumulated organically rich sediments due to high biological productivity and bottom

water anoxia [4,8,9]. Fluctuations in paleolake levels, driven by the interplay of tectonics and climate, have created conditions conducive to petroleum accumulation, as evidenced by discoveries in western Uganda [9–11]. This fluvial–lacustrine filled rift has emerged as a critical area for the study of the geological evolution of a petroleum system in a young rift basin setting, offering a contemporary analogue for understanding the maturation processes of lacustrine organic-rich source rocks in ancient rift lake basins [12,13]. Despite decades of intensive investigation into the Albert Rift and the broader EARS, a comprehensive understanding of its geological development and petroleum systems remains elusive [14–17]. Various research findings have yielded divergent perspectives on the mechanisms and timing of the rifting events [18–21], interactions between tectonics, and climate and sedimentation styles [9,22], as well as paleogeography and stratigraphy, e.g., [2,23–25]. Furthermore, while significant petroleum resources have been discovered through exploration efforts, uncertainties persist regarding the precise timing and nature of key elements within the petroleum system. Critical information regarding the nature of the source rocks essential for understanding hydrocarbon generation remains elusive. Current interpretations suggest potential sources within the Mid-Upper Miocene lacustrine intervals, particularly the Kasande Formation, yet analyses and correlations from drilled wells have not confirmed the effective source-rock facies associated with already-discovered oil and gas [17,26]. Consequently, assessments of the petroleum potential of this region remain speculative pending the identification of effective source rocks and a refined understanding of the petroleum system.

This study synthesizes both published and unpublished works in the literature, based on various sources, including Google Scholar, Science Hub, academic libraries, and government agencies. A detailed stratigraphic refinement of one of the least-studied regions, the Lake Edward and George area, was also conducted. This involved reviewing the relevant literature and well reports, analyzing seismic data and wireline logs, and integrating all the information to establish the subsurface stratigraphy of this area. Through this analysis, authors developed a tentative Albertine tectono-stratigraphy by considering the four type-localities in terms of event ages, underscoring the current pitfalls and contradictions within the different sources. A Basin and Petroleum Systems Modeling (BPSM) approach was also employed in the Onshore South Lake Albert Basin, where the available data allowed for reasonable predictions of the petroleum system elements. Despite the lack of confirmation as to the source rocks in this frontier rift basin, BPSM offers a powerful predictive tool which can be used to infer the petroleum generation, expulsion, and accumulation histories [27]. Such predictions will serve as critical milestones in advancing our understanding of the petroleum geology of this region until more definitive data become available. The objective of this study is to conduct a comprehensive analysis of existing geological data concerning the Albert Rift, focusing on its development and the implications for petroleum occurrences. The authors aim to identify current knowledge gaps, address some of these gaps through empirical and modeling approaches, and propose future research directions. By integrating previous findings with new insights, the study seeks to advance the understanding of the rift's petroleum potential and contribute to strategic exploration and resource management in this region. Through comprehensive integration, this paper presents a tectonostratigraphic framework and a petroleum system model for the Albert Rift, laying foundational groundwork for future refined models as our understanding evolves.

2. Materials and Methods

This section gives insights into the datasets, analytical tools, and methodologies employed to establish the tectono-stratigraphic framework and assess the hydrocarbon potential of the Albert Rift, Uganda. This study integrates seismic interpretation, well-log

analysis, geochemical characterization, and Basin and Petroleum System Modeling (BPSM) to evaluate key petroleum system elements. The primary datasets include 2D seismic data, well logs, and geochemical analyses of shale samples, which were processed and interpreted using industry-standard software. Schlumberger Petrel 2018 was used for seismic and well-log interpretation, Schlumberger PetroMod 2018 for BPSM, and Midland Valley's Move 2015 for structural restoration. Additionally, Rock Eval 7 Pyrolysis was conducted on shale samples to determine source-rock quality, thermal maturity, and hydrocarbon-generation potential. The results from Rock Eval were integrated with burial history and thermal maturity models to refine the basin's petroleum system evaluation. The workflow in this study follows a systematic approach, incorporating seismic stratigraphic analysis, structural restoration, source-rock evaluation, thermal maturity modeling, and hydrocarbon charge assessment, ensuring reliable predictions based on the petroleum history of this rift.

2.1. Developing a Tectonostratigraphic Framework

To develop tectonostratigraphic frameworks for different basins/sub-basins of the Albert rift, the available data, including both published and unpublished sources, were integrated for each particular basin/sub-basin. Particular emphasis was placed on the available seismic data, well logs, pre-drilling geological reports, well completion reports and outcrop data. For the Lake Edward–Lake George area, seismic data interpretation and well log analysis were carried out using the Schlumberger Petrel 2018 software. This approach helped identify and subdivide the entire stratigraphic section into categorical tectonostratigraphic units based on seismic and wireline responses. Additionally, mud-log data were integrated to enhance lithological characterization. The ages of the identified units were derived from palynological, molluscan, and vertebrate data provided by the Government of Uganda. These age assignments were constrained by documented tectonic events [2,22,24,25].

2.2. Petroleum Potential Evaluation

The petroleum potential evaluation was based on Basin and Petroleum Systems Modeling (BPSM) for the Southern Lake Albert Sub-basin, which contains the region's oldest known sedimentary sequences. The evaluation process included a detailed stratigraphic analysis, which served as the foundation for model inputs, followed by a geochemical assessment of potential source rocks, determination of boundary conditions, and model simulations and calibration. Data from one drilled well and a pseudo-well were used to support the evaluation process.

2.2.1. Southern Lake Albert Lithostratigraphic Reconstruction

A stratigraphic cross-section for the Southern Lake Albert Sub-basin was constructed by integrating the NW–SE seismic line presented by Simon et al. [25] and TRC well-log data. This cross-section illustrated the dipping strata towards the basin center. This generalized stratigraphic cross-section served as the basis for the placement of a pseudo-well (well X), establishing a crucial framework for Basin and Petroleum System Modeling (BPSM) in this data-limited region. The stratigraphic model provided essential input data, including formation thickness, lithology, and age, which are critical for modeling the depositional history, tectonic evolution, and interactions between petroleum system elements. These datasets form a comprehensive foundation for simulating hydrocarbon processes, such as maturation and generation, offering a detailed basis for the assessment of the region's petroleum potential.

2.2.2. Source-Rock Characterization

To assess the spatial and temporal variations in source-rock quality, Rock-Eval pyrolysis was performed on samples from two exploration wells, NGJ and KTB, using a Rock Eval 7 analyzer. These results, combined with geochemical data from the TRC well reports, facilitated an understanding of the source-rock characteristics and formed the basis for source-rock geochemical and kinetics inputs for the subsequent BPSM modeling stage. The TRC well samples exhibited an average total organic carbon (TOC) of 3.5% and a hydrogen index (HI) of 367 mg/g TOC, indicative of favorable petroleum source-rock conditions. These parameters were integrated into the BPSM for model input and calibration. Geochemical data, including TOC, HI, vitrinite reflectance (VR), and kerogen types from organic-rich shale facies of the Mid-Miocene intervals, were utilized to assess hydrocarbon potential.

2.2.3. Basin and Petroleum Systems Modeling

Basin and Petroleum Systems Modeling is a powerful tool used for evaluating temperature, source-rock maturity, and generation and migration of petroleum in sedimentary basins [28–30]. The 1D BPSM methodology is a fundamental approach in petroleum geology that models the geological and geochemical evolution of sedimentary basins along a single vertical profile. It helps researchers understand the timing of sediment deposition, compaction, and hydrocarbon generation by simulating the thermal and burial history over geological time. This methodology is essential for predicting the maturation levels of organic-rich source rocks and provides insights into hydrocarbon generation, expulsion, and migration [31–33]. By integrating various datasets, including stratigraphic, geochemical, and boundary data, 1D BPSM can enhance the accuracy and reliability of predictions, thereby reducing exploration risk. It is the most applicable tool where data is scarce, compared to more complex multi-dimensional models, serving as a preliminary guide and fundamental step towards more detailed and sophisticated 2D or 3D modeling efforts. Additionally, it allows for testing different geological scenarios and hypotheses, making it crucial for exploring and assessing hydrocarbon resources effectively. This method is performed using various software packages tailored for BPSM, including PetroMod (Schlumberger), Genesis-Trinity (Zetaware), and Permedia (Halliburton), among others. PetroMod is the most widely used in the petroleum industry due to its versatility [34]. PetroMod 1D can function independently or as an integrated part of the PetroMod 2D and 3D modeling systems. Single-point data, including wells and pseudo-wells, can be created from scratch, imported from the Well Editor, or extracted from PetroMod 2D and 3D models. In this study, Schlumberger PetroMod 1D was utilized to model an exploration well TRC and a pseudo-well X strategically located approximately 12 km apart. The stratigraphic dataset used for this modeling is detailed in Tables 1 and 2. After defining the stratigraphic dataset to be used in the model, the next step was to define the boundary conditions to be applied. Boundary conditions in PetroMod BPSM are critical for simulating thermal and pressure regimes in the basin over time. Parameters such as surface temperature, basal heat flow, paleo-water depth, and sediment–water interface temperature are assigned based on regional geological and geophysical studies. These values, often sourced from the literature or from measured data, are calibrated to match borehole temperature and vitrinite reflectance (Ro) trends. Proper boundary condition assignment ensures accurate modeling of heat transfer, maturation processes, and hydrocarbon generation. Boundary conditions, including surface temperatures and heat flow through time, were applied based on published heat flow data [35,36] and PetroMod-1D sea level curves, incorporating surface water interface temperatures specific to the locality (e.g., 24–25 °C for the Albert Rift). Geochemical data used in the modeling, including total organic carbon (TOC), hy-

drogen index (HI), and T_{max} and vitrinite reflectance (Ro) for both wells, were extracted from the TRC well reports. These are key parameters used to assess the source rock's hydrocarbon potential and its thermal maturity, which are critical for understanding the maturation and generation of hydrocarbons within a basin. TOC is a measure of the amount of organic material present in a source rock. A higher TOC indicates a greater potential for hydrocarbon generation, as organic matter is the primary source of petroleum. HI is a measure of the hydrogen content in the organic matter of a source rock. It provides insight into the type of hydrocarbons that may be generated, with higher HI values (typically > 300 mg HC/g TOC) indicating a dominance of Type I (oil-prone) kerogen, and lower values (typically < 300 mg HC/g TOC) suggesting Type II or III kerogen, which can produce gas or mixed gas–oil products. T_{max} helps to estimate the timing of hydrocarbon generation, as it indicates when the source rock reached the threshold for significant hydrocarbon generation (typically around 435 °C for oil generation). After these parameters were defined for the model, the next step involved simulations and calibrations performed with the aim of producing final results that matched the measured parameters. Calibration in PetroMod BPSM ensures the accuracy of the model by aligning simulation results with observed data. This process involves adjusting input parameters—such as heat flow, source-rock maturity, and stratigraphy—to match measured borehole temperatures, vitrinite reflectance (Ro), or other geochemical indicators. Iterative calibrations refine the model, enhancing the reliability of hydrocarbon-generation and migration predictions. This step is crucial for validating the geological and thermal history of the basin and achieving robust simulation outcomes. In this study, results of the simulation were calibrated against measured borehole temperature and vitrinite reflectance (Ro) trends from the TRC well. Iterative adjustments were made until an alignment was achieved between modeled and measured parameters. Burial-depth and time plots were overlaid with vitrinite reflectance modeled using the Easy %Ro method [36] embedded in the 1D Schlumberger 2018 PetroMod software. The decision to apply the measured geochemical parameters to the pseudo-well is based on the geological proximity of the wells, the lack of wells in the deeper western parts of this basin, and the assumption that these sections of the shale formation were deposited under similar lacustrine conditions. In Basin and Petroleum Systems Modeling (BPSM), actual drilled wells provide direct, high-precision subsurface data essential for calibration and validation, enabling accurate assessments of stratigraphy, lithology, and fluid properties, whereas pseudo-wells—derived from seismic data and other geophysical methods—are less reliable due to their indirect nature, lower resolution, and inherent uncertainties in seismic interpretation, often leading to potential inaccuracies in modeling; however, pseudo-wells remain valuable in data-sparse regions such as the Albert Rift for preliminary exploration and regional geological insights. In this study the pseudo-well was used to assess the lateral differences in petroleum system conditions in the deeper western parts of the basin where wells have not been drilled.

Table 1. Pakwach Basin lithostratigraphy.

Lithologic Unit	Age Description	Characteristics	Tectonic and Depositional Interpretation
Wangkwar Formation	Early Pliocene	Composed of fining-upward sequences starting with deposits dominated by conglomerates and coarse sands, and transitioning to fine sands. The upper portion consists of interbedded clays and fine sands.	Represents the initial phase of rifting in the Pakwach Basin, with block faulting creating half-graben structures and horst uplifts as primary sediment sources. Proximal alluvial fans formed near active fault scarps, with later fluvial systems transporting sediments basinward. The upper fine-grained deposits indicate decreasing depositional energy and ongoing subsidence.

Table 1. *Cont.*

Lithologic Unit	Age Description	Characteristics	Tectonic and Depositional Interpretation
Nyamusika Formation	Mid-Pliocene	Dominated by fine-grained, organic-rich sediments, including shales and fine sands interspersed with gastropod shells.	Represents the rift expansion stage with widespread tectonic subsidence. The extensive accommodation space favored lacustrine deposition under relatively stable tectonic conditions.
Paraa Formation	Late Pliocene to Early Pleistocene	Poorly sorted gritty sandstones, siltstones, and clays.	Reflects a renewed phase of active rifting, with intensified tectonic subsidence in the basin center and significant uplift along the rift shoulders. The depositional setting transitioned from lacustrine to fluvial, consistent with a falling-stage systems tract (FSST). Tectonic uplift influenced lake-level changes and sediment dispersal.
Tangi Formation	Mid-Pleistocene to Holocene	Coarse conglomerates, sands, and gritty clays near uplifted fault scarps.	Represents the late-stage rifting phase, marked by uplift, tilting of rift shoulders, and pronounced rift–floor subsidence. The formation captures the final stages of rift evolution, transitioning toward aggradational deposition as tectonic subsidence waned.

Table 2. Lithostratigraphy of Kaiso-Tonya/Central Lake Albert Basin.

Lithologic Unit	Age	Characteristics	Tectonic and Depositional Interpretation
Nondo Formation	Late Miocene to Early Pliocene	Basal conglomerates transitioning into sandstones and siltstones, culminating in deep lacustrine shales indicative of a maximum flooding surface.	Represents the first rifting phase with the development of the Kaiso-Tonya trough. Initial fluvial and deltaic systems delivered coarse sediments near basin margins, transitioning into deep lacustrine settings due to progressive subsidence.
Warwire Formation	Early to Mid-Pliocene	Alternating siltstones, sandstones, claystones, and coquina beds, with shell-rich coquinas indicating high-energy shallow lacustrine conditions.	Reflects intensified extensional faulting, base-level fall, and rapid sedimentation. Depositional environments transitioned from deltaic progradation during lake fluctuations to fluvial systems during extreme lowstands.
Kaiso Formation	Late Pliocene to Recent	This unit comprises claystones and siltstones, probably deposited as fluvial and floodplain fines near a shrinking lake shoreline.	Represents the final phase of rifting, with significant uplift of rift shoulders and episodic fault reactivation. Reduced accommodation space resulted in fluvial dominance and a waning lacustrine influence.

3. Results

This section presents the key findings from the literature, seismic interpretation, well-log analyses, geochemical characterizations, and Basin and Petroleum System Modeling (BPSM) of the Albert Rift, Uganda. These results provide insights into the tectonostratigraphic framework, structural evolution, source-rock potential, thermal maturity, and hydrocarbon-generation history of the study area.

3.1. Albert Rift Regional Tectonostratigraphy

The integrated analysis comprising seismic and well data, together with insights from the literature, reveals the tectonostratigraphic framework of the Albert Rift, highlighting the basin's stratigraphy, depositional environments, and tectonic phases. The results indicate a complex tectonostratigraphic evolution, driven by repeated extensional tectonics and subsidence, which controlled sedimentation patterns and the development of hydrocarbon plays across different sectors of the rift. The Albert Rift is divided, from north to south, into distinct sectors: Rhino Camp, Pakwach/Murchison Falls, Kaiso-Tonya/Central Lake Albert, Southern Lake Albert/Semliki Valley, and the Basins Area around Lakes Edward-George Basin. Each sector exhibits unique tectonic and depositional characteristics, contributing to the basin's petroleum potential. In this section we present the lithostratigraphy, and subsequently the tectonostratigraphy, of four of the five sectors, based on data availability.

The stratigraphic framework is derived from the integration of lithological characteristics from outcrops, seismic attributes, wireline log signatures, mud-log descriptions, faunal and palynological assemblages, and tephra data used for dating and correlation.

3.1.1. Tectonostratigraphy of the Pakwach Basin

The Pakwach Basin, dating from the Early Pliocene, is characterized by four distinct tectonostratigraphic units representing different rifting stages (Figure 3). These events are grounded in the lithostratigraphy, which is outlined in Table 1, along with a record of tectonic events.

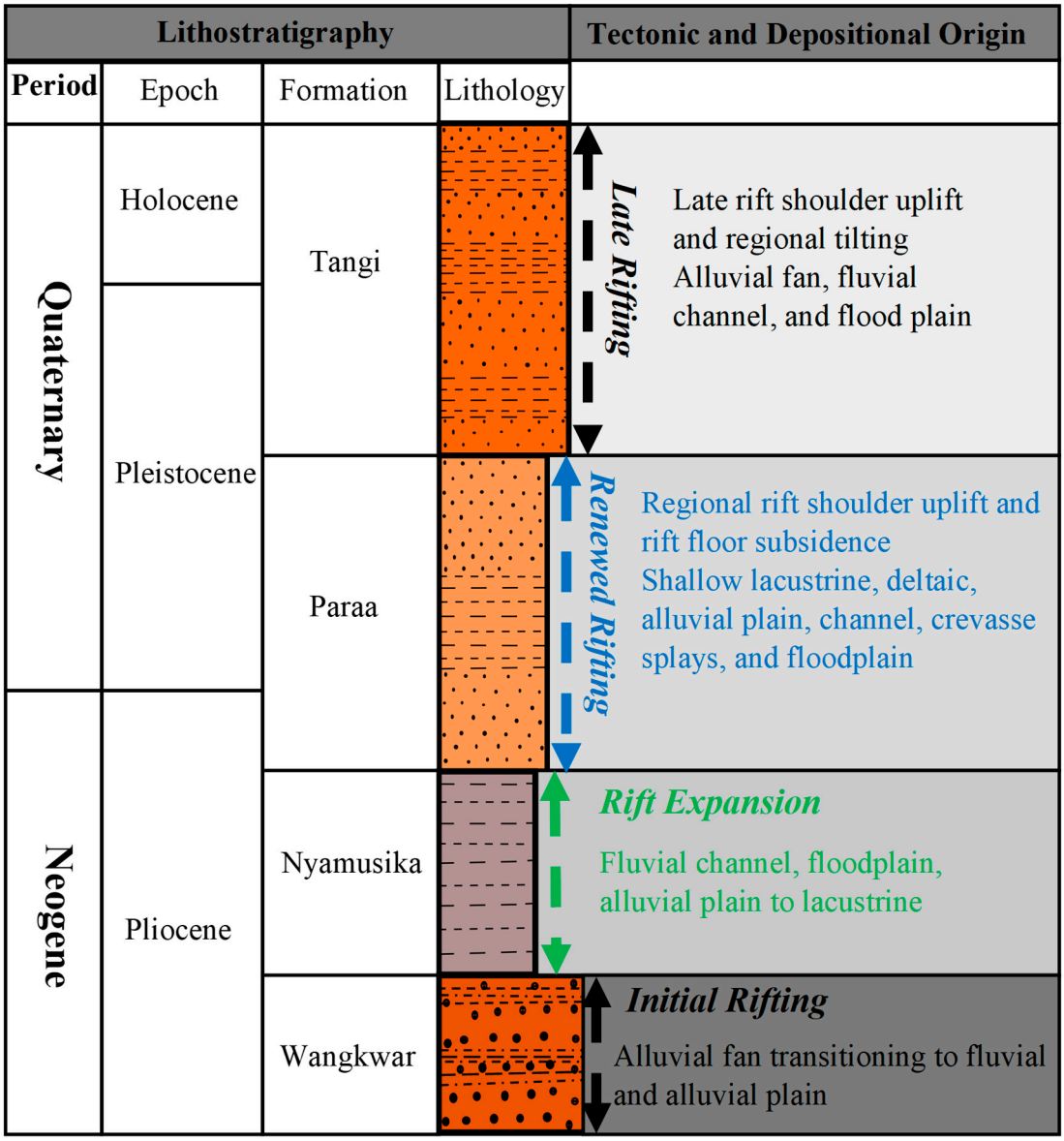

Figure 3. Generalized tectonostratigraphy of the Pakwach Basin.

Early Pliocene Rift Onset Phase

This earliest package marks the onset of rifting, with initial rift subsidence and sedimentation dominated by alluvial fan deposits transitioning to fluvial and alluvial plain systems. The sequence consists of coarse sands and conglomerates in the lower portion, shifting to finer sediments in the upper layers.

Mid-Pliocene Rift Expansion Phase

Deposition occurred during a phase of rift expansion, with associated slow subsidence across the basin. The sequence is dominated by lacustrine sediments, including shales and fine sands with gastropod shells, reflecting stable tectonic conditions and organic-rich sedimentation.

Late Pliocene to Early Pleistocene Renewed Rifting Phase

Renewed rifting and intensified subsidence resulted in the deposition of poorly sorted sediments in deltaic and shallow lacustrine environments. The unit features a mix of gritty sandstones, siltstones, and clays, with evidence of fluctuating lake levels and episodic sedimentation.

Mid-Pleistocene to Holocene Late Rifting Phase

The final phase of rifting, marked by significant uplift and subsidence, led to the deposition of high-energy alluvial fans and fluvial systems. The package consists of coarse sand, conglomerates, and gritty clays, indicating localized tectonic adjustments and an aggradational depositional environment.

Generally, the tectonostratigraphic evolution of the Pakwach Basin reflects a series of tectonic and depositional phases. The Early Pliocene marks the initiation of rifting, and is characterized by graben and half-graben structures and alluvial fan deposits. In the Mid-Pliocene, rift expansion facilitated lacustrine transgression, with fine-grained, organic-rich sediments found. During the Late Pliocene to Early Pleistocene, renewed tectonic activity resulted in fluvial–deltaic environments transitioning to shallow lacustrine settings. The Mid-Pleistocene to Holocene represents the latest stages of rifting, with pronounced uplift and high-energy alluvial fan and fluvial systems filling the newly created accommodation space. These findings highlight the tectonostratigraphic evolution of the Pakwach Basin, which has been shaped by dynamic tectonic and sedimentary processes.

3.1.2. Tectonostratigraphy of the Central Lake Albert Basin

The Kaiso-Tonya area, part of the Central Lake Albert Basin, exhibits a tectonostratigraphic evolution influenced by extensional tectonics, sedimentary infill, and fluctuating lake levels. The basin's development is characterized by three rifting phases, each marked by specific tectonostratigraphic units (Figure 4). This tectonostratigraphy is primarily based on the integration of lithostratigraphic interpretation (Table 2) and tectonic events.

Late Miocene to Early Pliocene Rift Initiation Phase

This phase involved the regional northward propagation of extensional faulting, leading to the development of the Kaiso-Tonya trough. The Nkondo succession records this phase, beginning with conglomerates indicative of high-energy deposition near fault scarps. It transitions to sandstones, siltstones, and deep lacustrine shales, reflecting the shift from fluvial and deltaic environments to a deep lacustrine setting, with a maximum flooding surface marking the transgressive-highstand phase.

Early to Mid-Pliocene Syn-Rift Base Level Fall

Intense extensional faulting during this phase led to base-level fall and erosion, with notable environmental stress, including a molluscan extinction event. The Warwire succession captures the geological record, and is characterized by alternating siltstones, sandstones, claystones, and coquina beds. These reflect shallow lacustrine, deltaic, and fluvial environments. Depositional shifts indicate active faulting, base-level changes, and sediment supply during fluctuating lake levels.

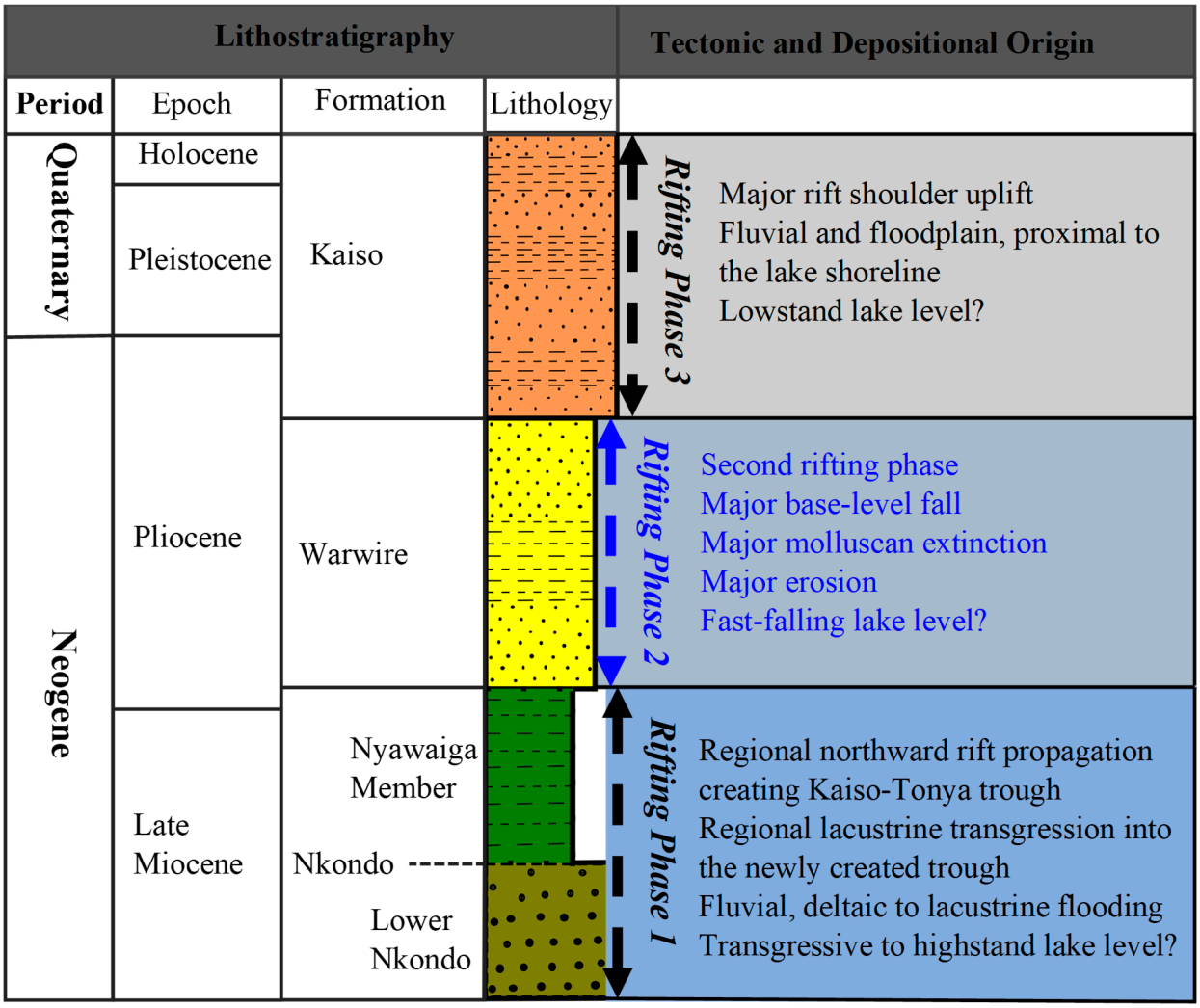

Figure 4. Generalized tectonostratigraphy of Central Lake Albert Basin.

Late Pliocene to Recent Rifting Phase

The final phase, marked by regional uplift of the Rwenzori massif in the south and rift shoulders, together with rift-floor subsidence, is represented by the Kaiso package, dominated by claystones and siltstones. These sediments reflect deposition in fluvial and floodplain environments near the shrinking lake shoreline, along with reduced accommodation space. The phase marks the transition from lacustrine systems to a primarily fluvial landscape.

3.1.3. Tectonostratigraphy of the Southern Lake Albert Basin

The Southern Lake Albert area, also commonly referred to as Semliki, exhibits four distinct tectonostratigraphic phases, interpreted based on documented sediment characteristics and regional correlations (Figures 5 and 6). This area forms the most studied area of the five basins/sub-basins, though its tectonics and stratigraphy are still not yet universally agreed upon. Nevertheless, we try to prepare a harmonized lithostratigraphy (Table 3) and subsequent tectonostratigraphy from the documented data, which will form a foundation for future refinements, e.g., [15,16,22,24,25].

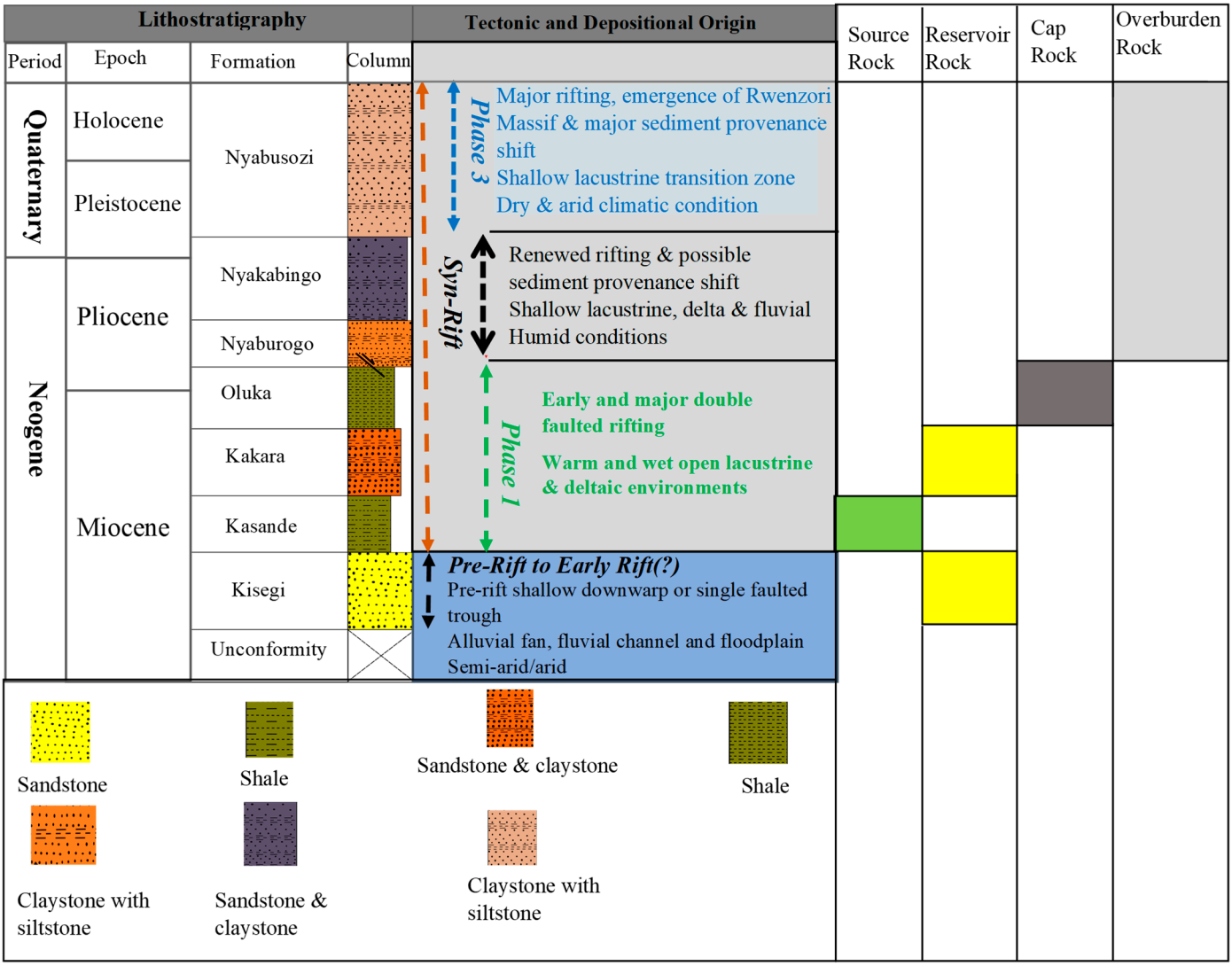

Figure 5. Generalized tectonostratigraphy of Southern Lake Albert Basin.

Table 3. Lithostratigraphy of Semliki/Southern Lake Albert Basin.

Lithologic Unit	Age	Characteristics	Tectonic and Depositional Interpretation
Kisegi Formation	Early Miocene	Conglomerates grading into channel cross-bedded sandstones, with thin interbeds of clay, tuff, and gypsum. Gypsum stringers fill cracks due to tectonic stress.	Represents the transition from pre-rift to early rift sedimentation in an arid climate. Deposited in proximal alluvial fan and braided river environments, with localized floodplain deposition. Evaporitic gypsum layers indicate a hot, dry climate with active tectonic stress.
Kasande Formation	Mid-Miocene	Dark brown to yellow-brown mudstones interbedded with channel sandstones and capped by two prominent black coaly shale intervals. Geophysical logs reveal organic-rich deposits.	Deposited in a warm, wet, open lacustrine setting. The coaly shales indicate stagnant water conditions in marshes, swamps, and mudflats. Represents an organic-rich interval interfingered with nearshore lacustrine deposits.
Kakara Formation	Late Miocene	Coarsening-upward sequences transitioning to fining-upward cycles. Iron-rich sandstones and ironstone layers at the base indicate shifting depositional energy.	Reflects deltaic and shallow lacustrine environments under humid climatic conditions. The ironstone layers indicate reduced accommodation space with increased fluvial influx, while cyclicity reflects fluctuations in base level.

Table 3. *Cont.*

Lithologic Unit	Age	Characteristics	Tectonic and Depositional Interpretation
Oluka Formation	Late Miocene to Early Pliocene	Dark shale at the base, overlain by conglomeratic ironstone, interbedded claystones, shales, siltstones, and sandstones. Concretionary ironstone and silica-cemented sandstones present.	Represents deltaic, mudflat, and lacustrine settings influenced by episodic tectonics and climatic changes. Sharp gamma-ray increases in logs indicate significant shifts in depositional energy.
Nyaburogo Formation	Early Pliocene	Silicified basal layer, thick claystones interbedded with rust-brown to yellowish-brown siltstones and pisolitic ironstones.	Reflects deposition in delta plain, prodelta, and shoreline settings, shaped by fluctuating depositional energy. The silicified beds mark renewed rifting, while overlying claystones indicate low-energy lacustrine conditions.
Nyakabingo Formation	Late Pliocene	Thick lacustrine shale horizon at the base, followed by coarsening-upward cycles of light gray to greenish-gray claystones, iron-stained siltstones, and pebbly sandstones. Carbonate nodules and capping ironstone layers present.	Represents floodplain, lagoonal, and lacustrine deposition under humid conditions. The basal shales reflect a deep lake setting, transitioning to higher-energy fluvial and floodplain deposition due to increased sediment supply. Carbonate nodules suggest fluctuating water levels.
Nyabusozi Formation	Early Pleistocene to Present	Massive sandstone at the base with low gamma-ray response, overlain by alternating sands and clays interbedded with eight ironstone layers.	Captures the transition driven by uplift of the Rwenzori Massif, altering lake dynamics and sediment provenance. Reflects lacustrine and shoreline environments influenced by fluctuating lake levels, tectonic uplift, and climate variability.

Early Miocene Rift Initiation Phase

The sedimentary package representing this phase marks the onset of rifting, with coarse-grained, poorly sorted basal conglomerates, dominant channel sandstones, and thin floodplain clays, reflecting alluvial fan and braided to meandering river deposition under an arid climate. Tensional gypsum stringers indicate active tectonic stress during this early phase or later tensional tectonics.

Mid- to Late-Miocene Major Rifting Phase

This package represents a major syn-rift rifting phase that resulted in the deposition of lacustrine, deltaic, and fluvial sediments. It marks the transition from a fluvial basin to a lacustrine basin. This sedimentary package has been differentiated into three distinct formations. The Kasande succession, which marks the earliest rifting unit, is composed of organic-rich mudstones and coaly shales, and is thought to have been deposited in a warm, wet, open lacustrine environment, while the overlying Kakara beds comprise deltaic and shallow lacustrine sediments with iron-oxide-rich sandstones, reflecting fluctuating depositional energy. Marking the end of this package, the Oluka Formation was deposited in deltaic, mudflat, and lacustrine settings, with ironstone and silica-cemented sandstones indicating fluctuating conditions influenced by tectonics and climate.

Early to Late Pliocene Syn-Rift Phase

This package represents a tectonostratigraphic phase that resulted in a shift in sediment provenance due to changes in the sediment routing systems, shifts primarily caused by interruptions in the drainage flow directions. This package is subdivided into the Nyaburogo and Nyakabingo lithostratigraphic units, which document alternating deltaic, lacustrine, and prodelta depositions. The lower section of this package is represented by the Nyaburogo unit, which is characterized by a silicified basal layer, followed by thick sequences of claystones interbedded with rust-brown to yellowish-brown siltstones and pisolitic ironstones. Overlying this unit is the unit which marks the transition from low-energy shallow lacustrine to higher-energy fluvial environments, with carbonate nodules and ironstones marking fluctuating water levels and episodic sedimentation.

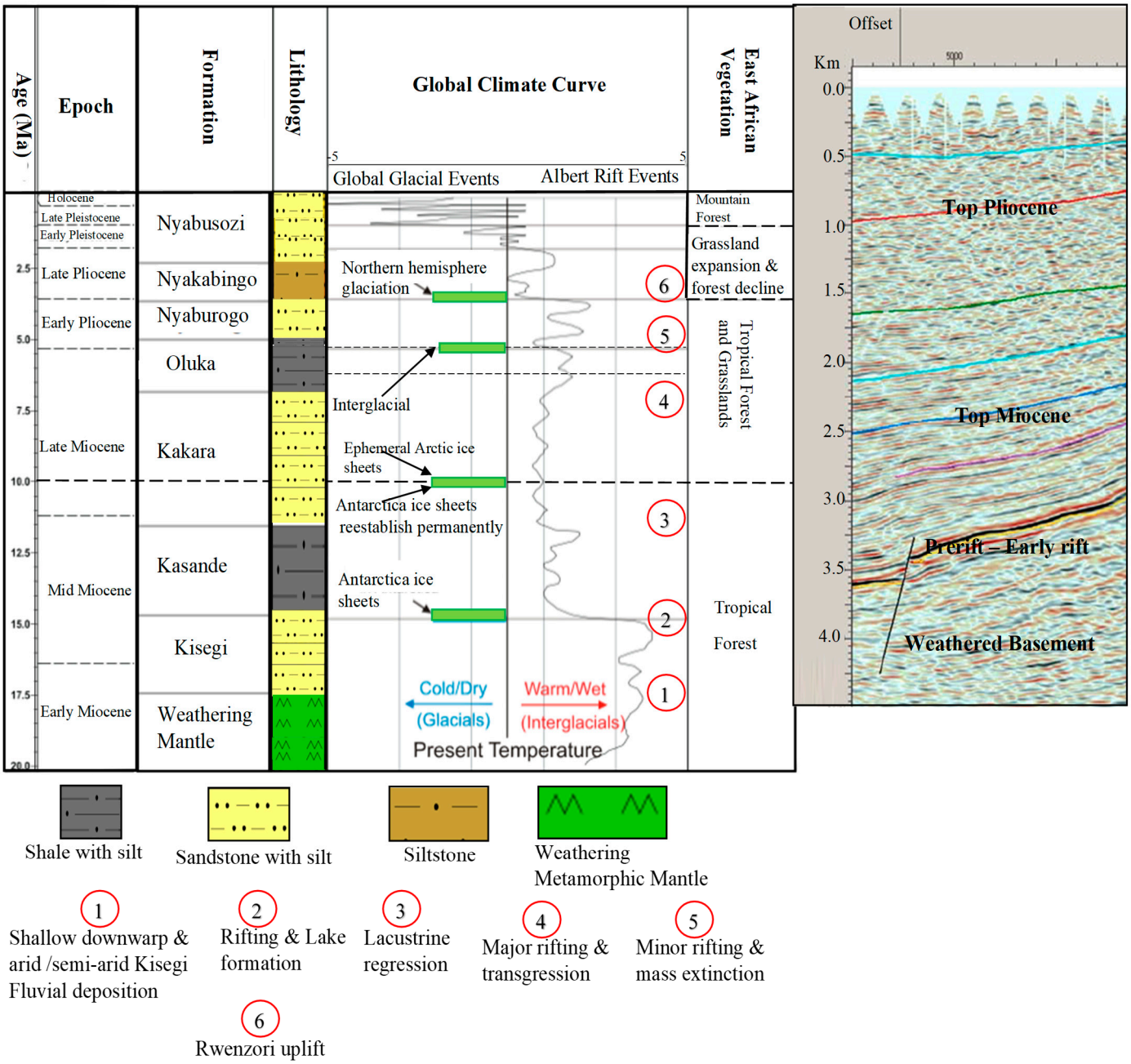

Figure 6. Generalized geological and climatic events chart for the Southern Lake Albert Sub-basin (Semliki) that represents the most complete stratigraphy of the rift sediments. The climate curve is based on Frakes [37] and Hardenbol et al. [38].

Early Pleistocene to Present Rifting Phase

The period from the Early Pleistocene to the present marks a transitional phase in the basin's evolution, driven by the uplift of the Rwenzori Massif, which split the regional lacustrine basin into two distinct basins, altered sediment provenance, and triggered molluscan changes; this period is captured in the Nyabusozi Formation, characterized by a basal massive sandstone layer with low gamma-ray response overlain by alternating sands and clays interbedded with ironstone layers, reflecting dynamic depositional processes in lacustrine and shoreline environments influenced by fluctuating lake levels, tectonic uplift, and climatic variability.

Overall, the southern Lake Albert Basin represents the most complete sedimentary fill and records all the known tectonic and climatic shifts since the early Miocene (Figure 6).

3.1.4. Tectonostratigraphy of the Basin Area of Lakes Edward-George Basin

Analysis of seismic data, wireline well logs, mud-logs, and other preliminary information shows that the tectonostratigraphy of the Lakes Edward–George Basin is characterized by three progressive rifting phases, each influencing sedimentation patterns and structural development. The lithostratigraphic information developed by interpretation from these datasets is presented here (Table 4), along with the tectonostratigraphic chart (Figure 7).

Table 4. Lithostratigraphy of the Edward Basin.

Lithologic Unit	Age	Characteristics	Tectonic and Depositional Interpretation
Edward Formation	Late Miocene to Late Pliocene	Poorly sorted, angular, immature sandstones; fluvial systems with braided rivers.	Onset of continental rifting; extensional tectonics, lithospheric stretching, and faulting leading to proximal sedimentation with limited transport distances.
Ngaji Formation	Late Pliocene to Pleistocene	Sandstones (fluvial, alluvial plains, deltas); claystones and siltstones (lacustrine).	Active rift expansion and subsidence; development of horst and graben structures, leading to diverse sedimentation in fluvial, deltaic, and lacustrine environments.
Bwambara Formation	Pleistocene to Holocene	Loose quartz sands with shell fragments; alluvial fans, braided river systems, fan deltas.	Late rift stage; tectonic uplift of rift shoulders and fault block rotation, resulting in high-energy sedimentation with reduced accommodation space.

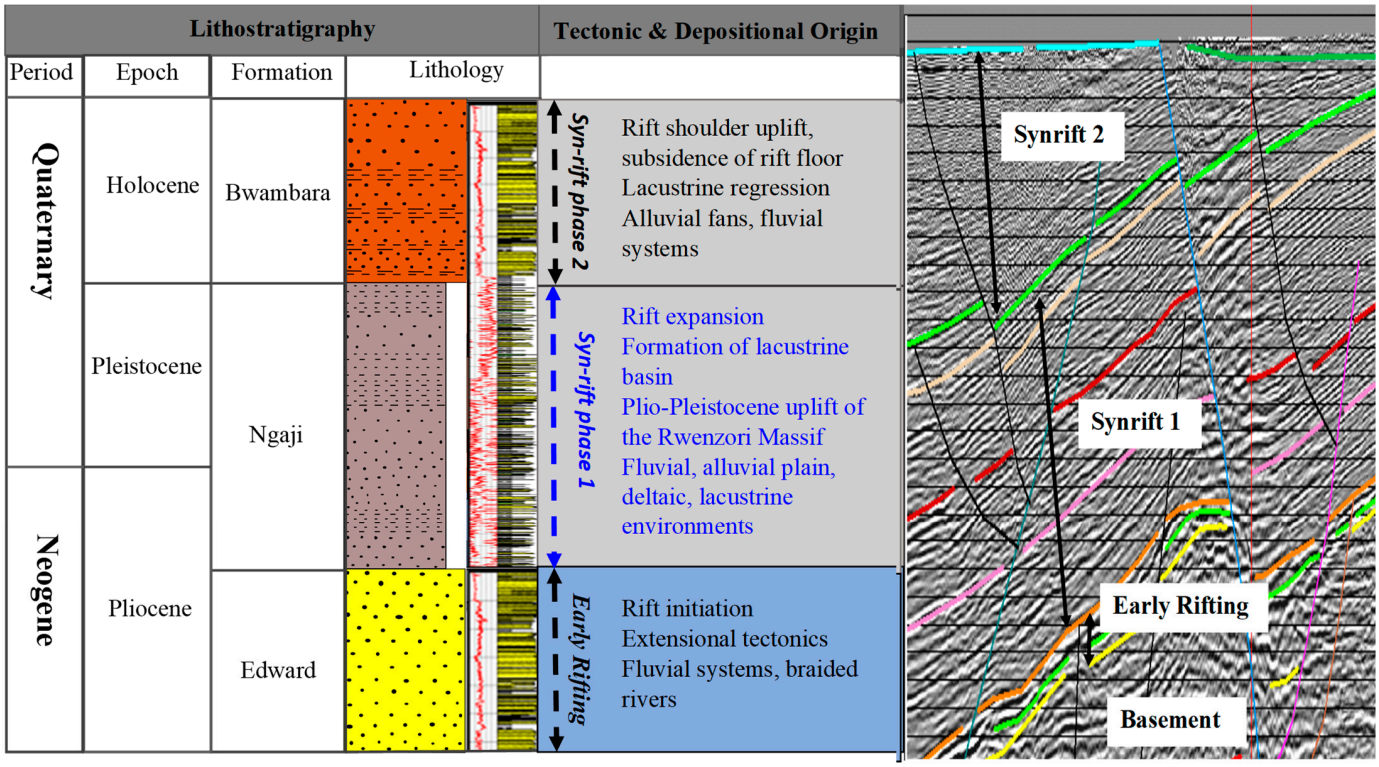

Figure 7. Generalized tectonostratigraphy of the Lakes Edward–George Basin.

Pliocene Early Rifting Phase

The Early Rifting Phase reflects the onset of rifting, and is characterized by extensional tectonics and the development of normal faults, accompanied by localized rift-floor and rift-margin volcanic activity. Sedimentation during this period was dominated by fluvial systems, with braided rivers transporting poorly sorted, angular, and immature sandstones derived directly from uplifted rift shoulders, indicative of proximal deposition with limited transport distances. The depositional environment, shaped by active faulting and limited accommodation space, highlights the interaction between tectonic uplift and sediment delivery, marking the initial phase of rift basin development.

Late Pliocene to Pleistocene Syn-Rift Phase

This Syn-Rift Phase marks a period of active rift expansion characterized by continued basin extension, subsidence, and the development of horst and graben structures through enhanced normal faulting. This tectonic activity created substantial accommodation space, leading to diverse sedimentation, with fluvial systems depositing sandstones on alluvial plains and deltas at the basin margins, while quieter lacustrine settings in the central basin accumulated finer-grained claystones and siltstones. The depositional variability reflects a rift expansion stage in which tectonic controls and fluctuating sediment supply shaped the interplay between fluvial, deltaic, and lacustrine environments.

Pleistocene to Holocene Late Syn-Rift Phase

The most recent Syn-Rift Phase signifies a late rift stage marked by continued uplift of rift shoulders alongside rift-floor subsidence and creation of new accommodation space. Lithologically, loose quartz sands with shell fragments indicate deposition in higher-energy environments influenced by episodic flooding and proximity to lacustrine conditions. Dominated by alluvial fans at the basin margins and braided river systems feeding fan deltas, this phase reflects proximal, high-energy sedimentation driven by renewed tectonic activity.

3.2. Petroleum Potential of the Albert Rift

An integrated analysis of the available geological, geochemical, and geophysical data highlights the Southern Lake Albert area, particularly the Semliki Sub-basin, as a key region of hydrocarbon prospectivity. This area is characterized by the presence of the oldest sedimentary sequences within the Albert Rift, coupled with mature source rocks that have generated, and continue to generate and expel, associated hydrocarbons.

This section delves into the stratigraphic framework of the Southern Lake Albert area, evaluating source-rock geochemical data to establish the richness, maturity, and hydrocarbon-generation potential of key formations. Furthermore, the timing and processes of petroleum generation and expulsion are presented, emphasizing their implications for potential hydrocarbon accumulations in the sub-basin and the entire Albert Rift as a whole.

3.2.1. South Lake Albert Lithostratigraphy

The NW–SE cross-section along line A-B (Figure 2), generated from seismic and well data using the Midland Move 2015.1 software for the southern Lake Albert Basin, demonstrates a northwestward deepening and thickening of the basin and its stratigraphic units away from the rift margin in the southeast (Figure 8). This pronounced feature is primarily attributed to neotectonic faulting. Additionally, the cross-section reveals the interplay of extension and compression, a phenomenon which results in both a thinning and a thickening of the strata. From the integration of this cross-section, well reports, and published data, the stratigraphic results were obtained, as presented in Tables 5 and 6.

Table 5. Stratigraphic dataset obtained from the published literature and well reports used to model the burial, thermal, and hydrocarbon-generation history of the rift at exploration well TRC.

Layer	Age From (Ma)	To (Ma)	Thickness Top (m)	Base (m)
Nyabusozi	0	2.5	0	848
Nyakabingo	2.5	3.8	848	1055
Nyaburogo	3.8	4.8	1055	1492
Oluka	4.8	7	1492	1883

Table 5. *Cont.*

Layer	Age From (Ma)	To (Ma)	Thickness Top (m)	Base (m)
Kakara	7	11.9	1883	2425
Kasande	11.9	14	2425	2540
Kisegi	14	17	2540	3600

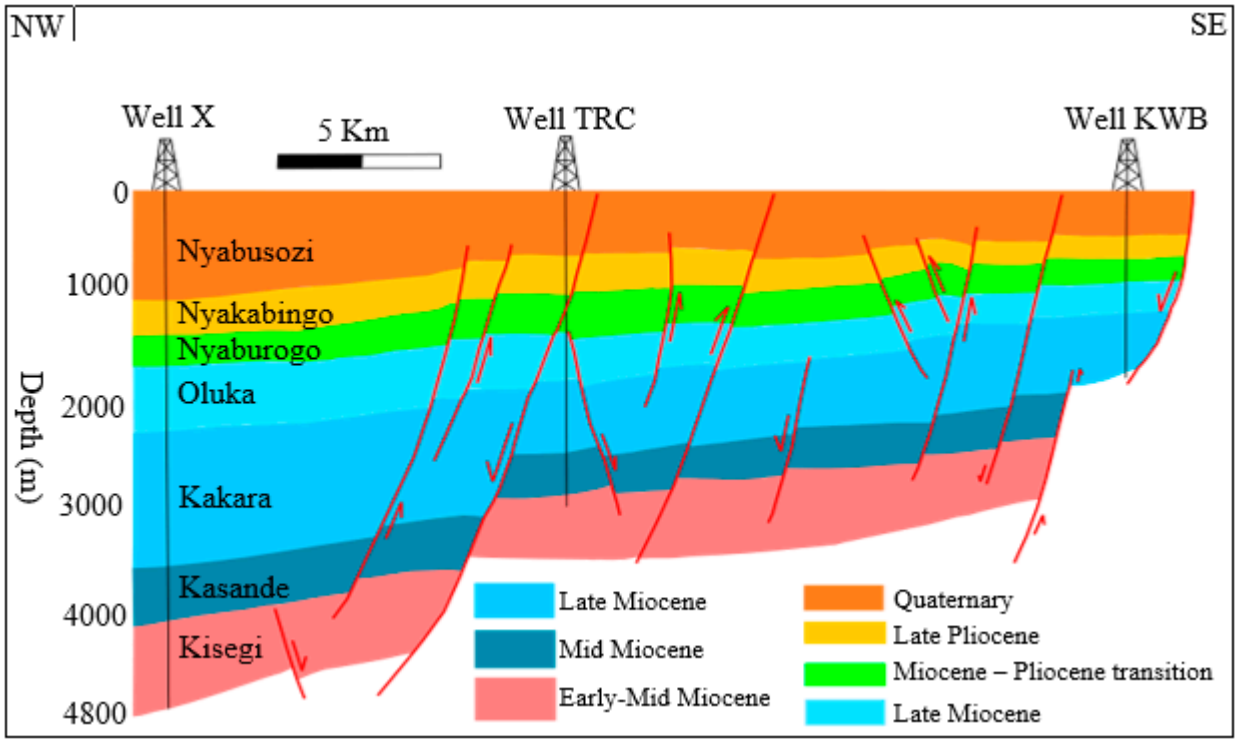

Figure 8. Simplified stratigraphic cross-section along the NW–SE direction showing different formations penetrated by wells.

Table 6. Stratigraphic dataset derived from the integration of TRC well data with previous seismic interpretations used to model the burial–thermal and hydrocarbon-generation history of the rift at pseudo-well X.

Layer	Thickness Top (m)	Bottom (m)	Age Top (Ma)	Bottom (Ma)
Nyabusozi	0	1056	0	2.5
Nyakabingo	1056	1392	2.5	3.8
Nyaburogo	1392	1632	3.8	4.8
Oluka	1632	2208	4.8	7
Kakara	2208	3456	7	11.9
Kasande	3456	4008	11.9	14
Kisegi	4008	4800	14	17

3.2.2. Source-Rock Characteristics

Analysis of the Rock-Eval pyrolysis data revealed crucial parameters indicative of organic richness, thermal maturity, and depositional environment. The parameters include the total organic carbon (TOC) content; S1 and S2 peak areas, representing free and kerogen-bound hydrocarbons, respectively; and T_{max} values reflecting thermal maturity. Additionally, the hydrogen index (HI) offers insights into the type and quality of organic

matter and the presence of mineral matter. These parameters collectively provide a comprehensive understanding of the organic composition and thermal history of the analyzed samples. These parameters are provided in the respective tables and plots for each well.

In the NGJ well, the total organic carbon (TOC) contents range from 0.11% to 0.48%. Hydrogen index (HI) values vary between 9 mgHC/g TOC and 123 mgHC/g TOC. T_{max} values range from 345 °C to 424 °C. Additionally, the S1 and S2 values are in the ranges of 0.00–0.03 mg/g and 0.02–0.6 mg/g, respectively. The samples also exhibit production index (PI) values ranging from 0.01 to 0.32 (Table 7).

Table 7. Rock-Eval pyrolysis data for the NGJ shale samples.

Depth (m)	Quantity (mg)	TOC (%)	S1 (mg/g)	S2 (mg/g)	T_{max} (°C)	TpkS2 (°C)	PI	HI
1146–1149	46.9	0.22	0	0.02	404	441	0.10	9.00
1152–1155	52.8	0.18	0	0.09	421	457	0.03	49.00
1164–1167	57.8	0.20	0.01	0.04	345	382	0.28	19.00
1167–1170	53.4	0.15	0	0.03	418	455.00	0.12	17.00
1257–1260	46.7	0.48	0.01	0.6	413	450	0.01	123.00
1440–1443	53.8	0.39	0	0.46	421	458	0.01	116.00
1461–1464	58.9	0.25	0.01	0.17	422	458	0.05	69.00
1473–1476	53.9	0.19	0.02	0.11	424	461	0.14	59.00
1482–1485	54.7	0.18	0	0.03	403	440	0.09	14.00
1491–1494	59.6	0.11	0.01	0.03	415	452	0.32	27.00
1530–1533	49.6	0.19	0.01	0.12	382	419	0.04	62.00
1545–1548	44.9	0.13	0	0.02	354	391.00	0.15	14.00
1551–1554	45.8	0.14	0.01	0.04	411	448	0.12	30.00
1563–1569	55.3	0.28	0.03	0.17	414	451	0.14	61.00

In the KWB well, the total organic carbon (TOC) contents range from 0.17% to 0.68%. Hydrogen index (HI) values vary within the range of 28–259 mgHC/g TOC. T_{max} values range from 403 °C to 433 °C. Additionally, the S1 and S2 values are in the ranges of 0.00–0.21 mg/g and 0.05–1.75 mg/g, respectively. The samples also exhibit production index (PI) values ranging from 0.02 to 0.13 (Table 8).

Table 8. Rock-Eval pyrolysis data for the KWB shale samples.

Depth (m)	Quantity (mg)	TOC (%)	S1 (mg/g)	S2 (mg/g)	T_{max} (°C)	TpkS2 (°C)	PI	HI
1467.00	50.8	0.24	0.02	0.23	407	444	0.07	98
1476.00	44.9	0.22	0.01	0.21	414	451	0.07	97
1482.00	58.4	0.29	0.01	0.26	419	456.00	0.03	88
1518.00	41.9	0.17	0.00	0.06	418	455	0.06	33
1524.00	55.4	0.31	0.01	0.26	412.00	449.00	0.03	83
1530.00	60.8	0.30	0.02	0.36	414	451	0.06	120
1554.00	52.2	0.67	0.02	0.61	433	470	0.04	92
1569.00	61.4	0.35	0.03	0.4	413.00	450.00	0.06	115
1578.00	42.8	0.19	0.00	0.05	422	458	0.07	28
1581.00	60.6	0.43	0.05	0.85	421	458	0.05	199
1584.00	58.9	0.68	0.21	1.75	420	457	0.11	259
1629.00	57.6	0.44	0.15	1.03	411	448	0.13	232
1650.00	44.8	0.48	0.02	0.84	415	452.00	0.02	173

Table 8. *Cont.*

Depth (m)	Quantity (mg)	TOC (%)	S1 (mg/g)	S2 (mg/g)	T_{max} (°C)	TpkS2 (°C)	PI	HI
1827.00	52.3	0.27	0.01	0.22	416	453	0.03	80
1839.00	54.9	0.19	0.01	0.16	403	440	0.05	86
1851.00	50.8	0.25	0.02	0.31	415	451.00	0.05	125
1866.00	54.2	0.37	0.02	0.56	413	450.00	0.03	152
1875.00	54.1	0.39	0.06	0.68	419	455	0.08	173
1887.00	44.9	0.41	0.10	0.7	409	445	0.12	171

Based on the tables and cross plots, the NGJ samples fall within the poor and gas-prone organic matter zones (Figure 9a,b), while the KWB samples plot in the poor and fair gas-prone zones, albeit skewed towards poorness (Figure 10a,b).

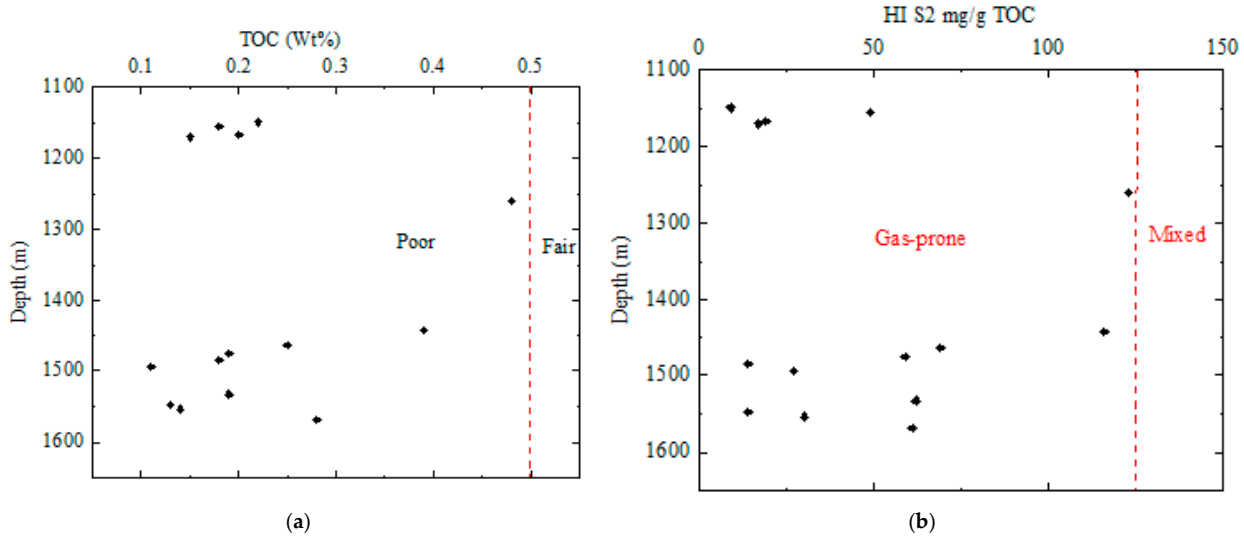

Figure 9. (**a**) TOC versus depth and (**b**) HI versus depth plots based on Dembicki [39] for the Pliocene shale samples selected from NGJ borehole cuttings.

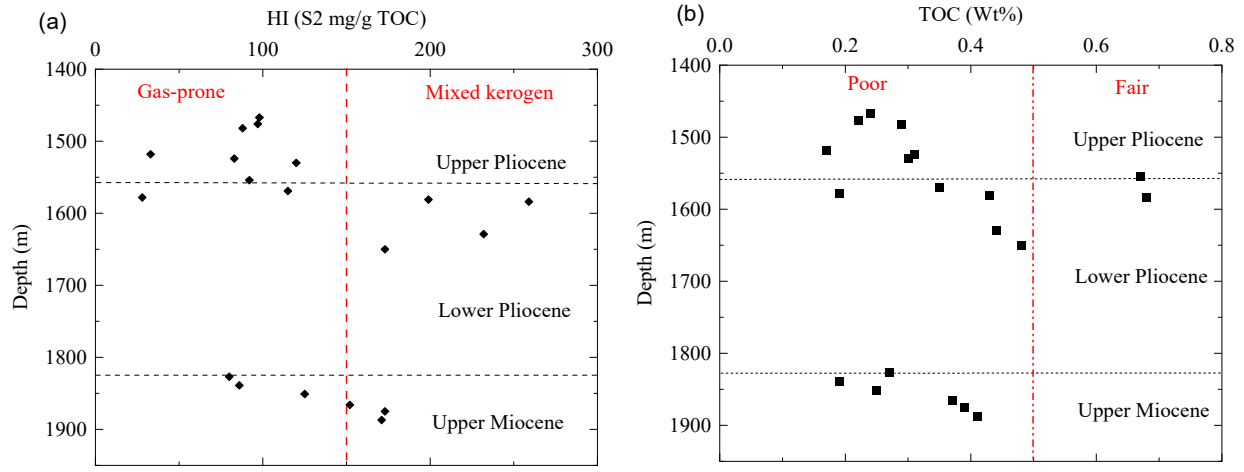

Figure 10. (**a**) TOC versus depth and (**b**) HI versus depth plots for Miocene–Pliocene shale samples selected from KWB borehole cuttings.

Conversely, the plots for the data picked from TRC well reports fall within the mixed fair, good, and very good categories based on the classification of Dembicki [39], with organic matter displaying tendencies towards the categories of oil-proneness, mixed, and gas-proneness (Figure 11a–d).

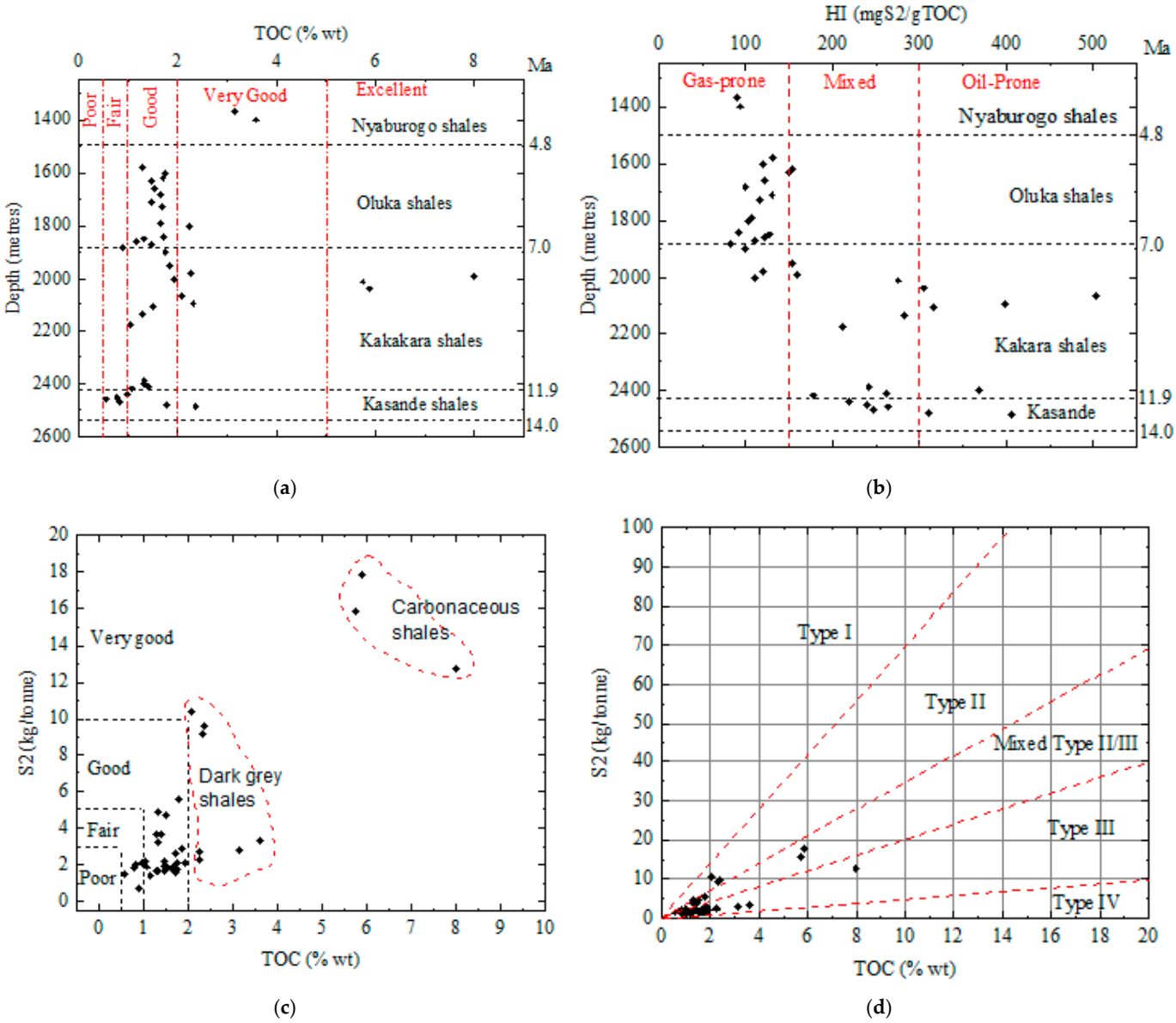

Figure 11. (**a**) TOC versus depth, (**b**) HI versus depth, (**c**) S2 versus TOC for generation potential classification, and (**d**) S2 versus TOC for organic matter type classification plots for Miocene shales of the TRC well utilizing information obtained from well reports provided by the Ministry of Energy and Mineral Development, Uganda (after Dembicki [39]).

3.2.3. Burial and Thermal History

The burial history curves for the TRC well reveal four distinct subsidence phases, while pseudo-well X shows five distinct phases. The first phase exhibits slow subsidence rates from the Mid-Miocene to the beginning of the Upper Miocene. This is followed by increased subsidence rates from the Upper Miocene to the Early Pliocene. The Early to Late Pliocene witnessed a slower subsidence rate compared to the previous phase, which was then followed by an accelerated subsidence throughout the Pleistocene (Figures 12 and 13). Pseudo-well X follows the same trend, although with five phases.

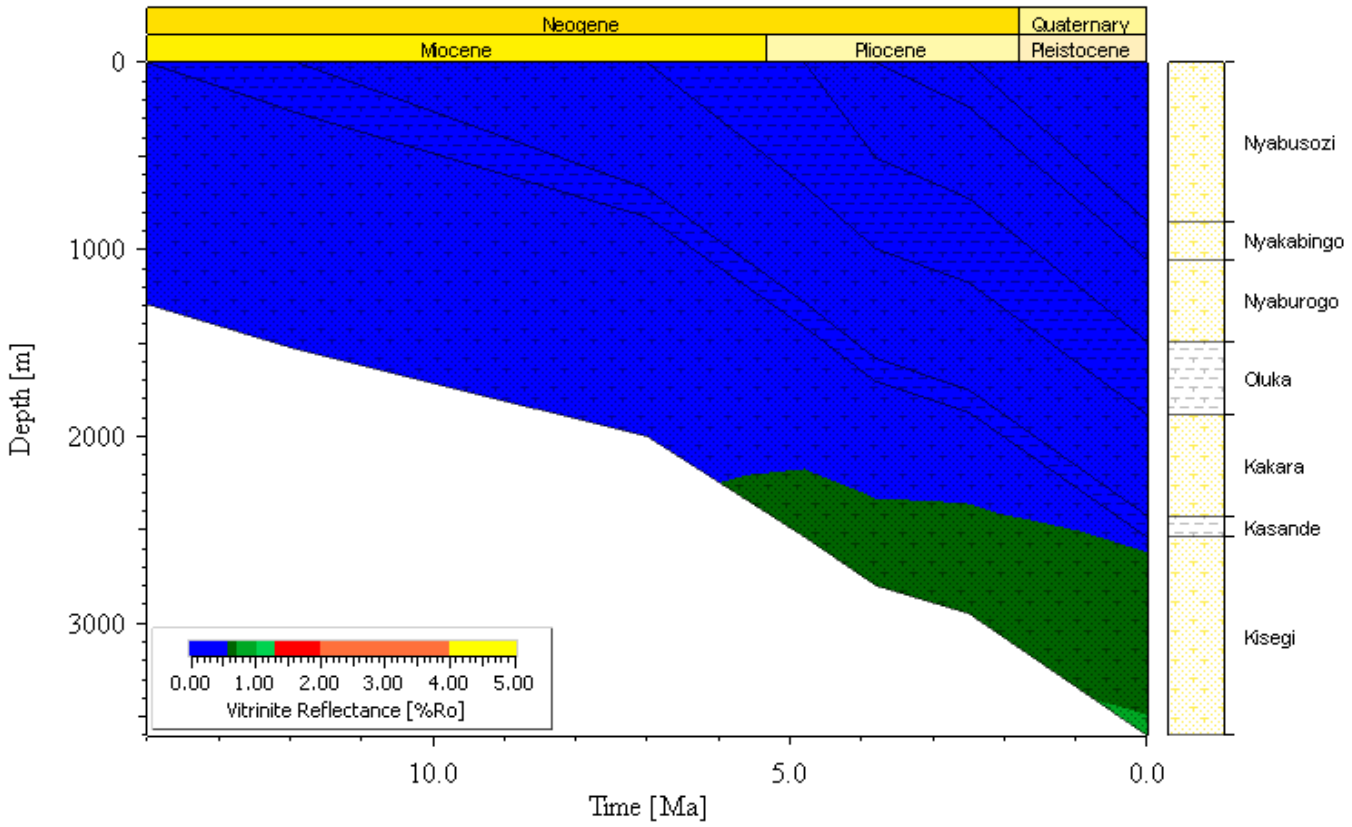

Figure 12. Burial history for the exploration TRC well.

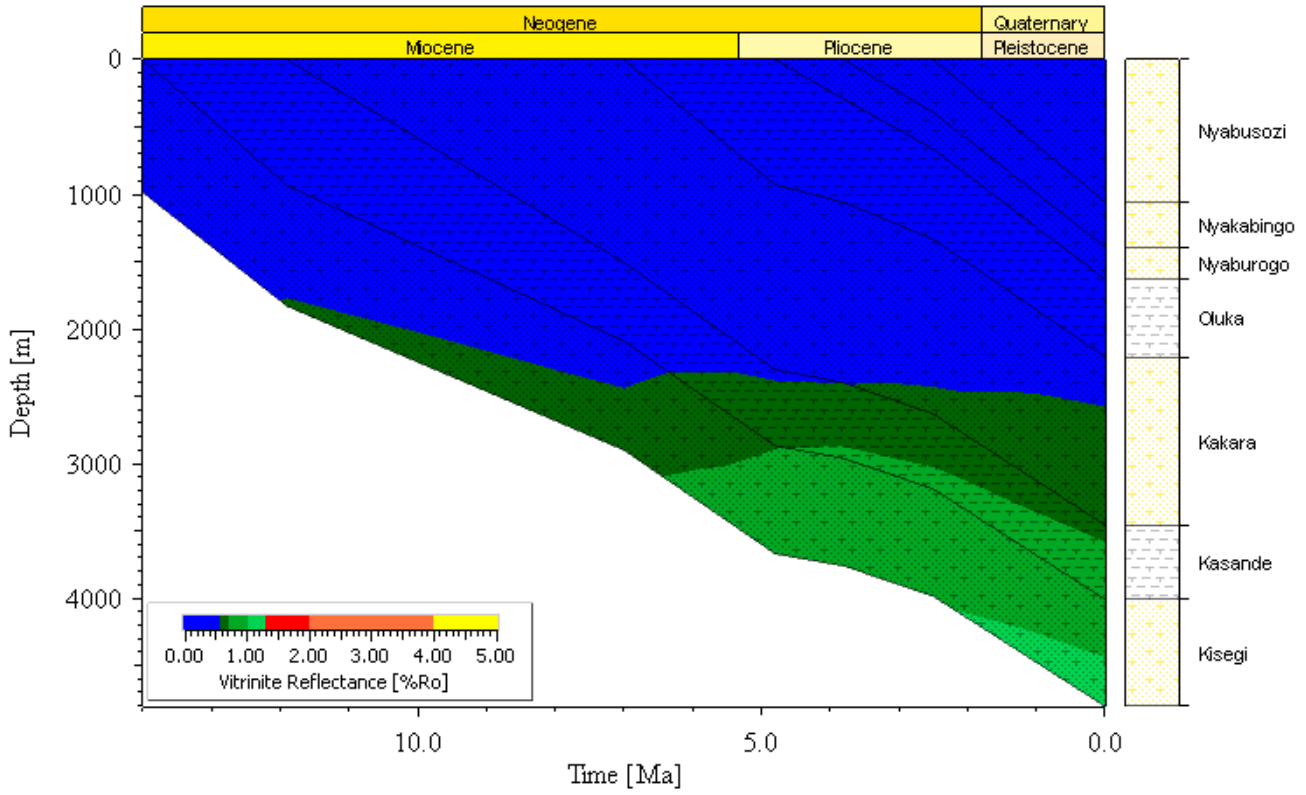

Figure 13. Burial history for pseudo-well X.

Regarding thermal maturity, in well TRC, at the top of the lacustrine shale source rock (2425 m), the Vr is 0.50% Ro, while at the base of the source rock (2540 m), the Vr is 0.53% Ro (Figure 14b). These Vr values indicate that the source rock is in the early stages of oil generation and approaching the onset of peak oil generation. For pseudo-well X, the top of the source rock (3456 m) shows a Vr value of 0.66% Ro, while the base of the source rock (4008 m) has a Vr value of 0.84% Ro (Figure 15). These values indicate the source rock is in the late stages of peak oil generation.

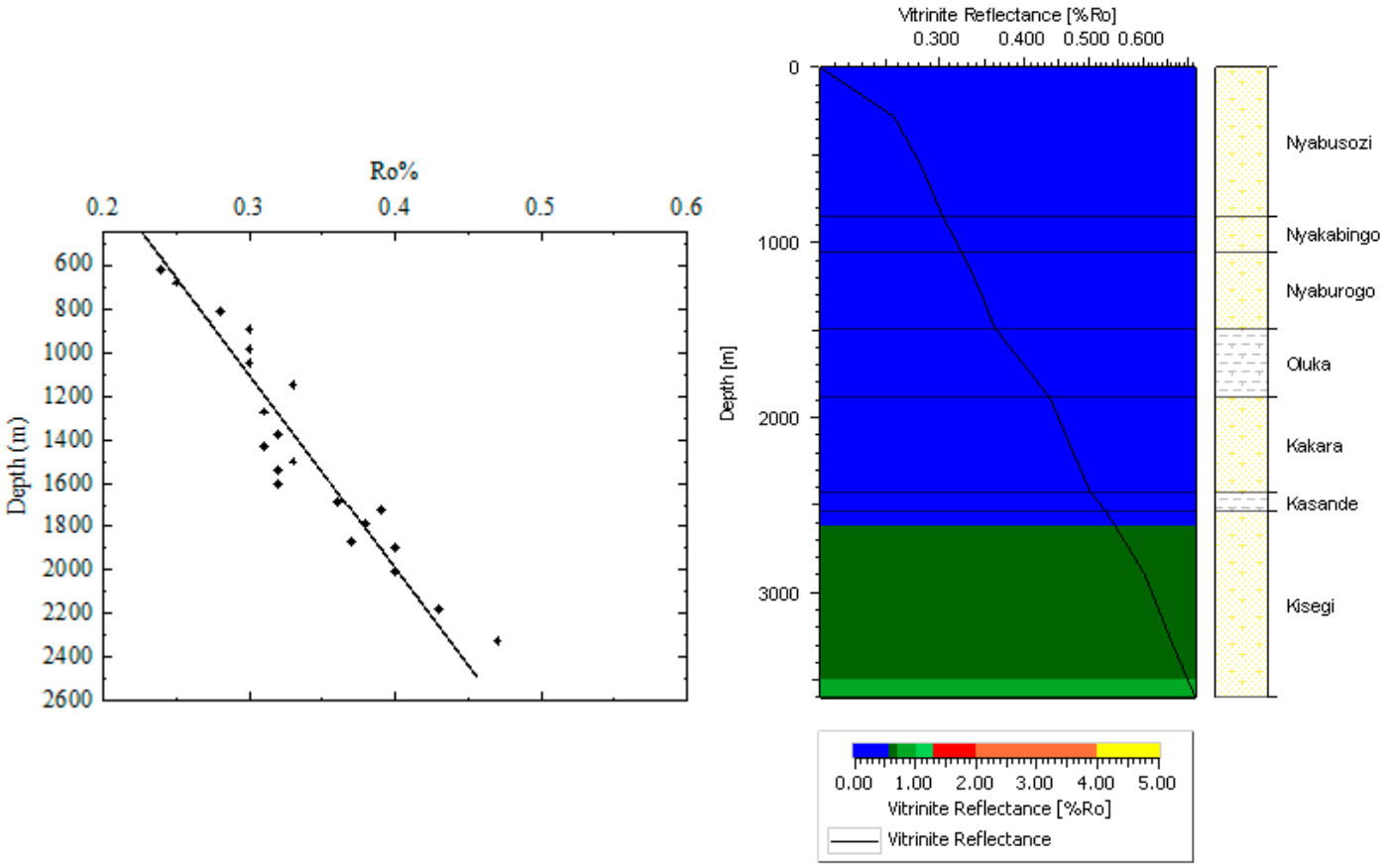

(**a**) (**b**)

Figure 14. Comparison of (**a**) measured and (**b**) modeled vitrinite reflectance for well TRC.

3.2.4. Hydrocarbon Transformation

The modeling results for the two wells reveal distinct transformation and hydrocarbon-generation histories as sediments deepen towards the depocenter in the northwest. For the TRC well, the transformation of kerogen into hydrocarbons is minimal, with a current transformation ratio (HTR) of approximately 0.2% to 0.3% (Figure 16a). At well X, located 12 km northwest of the TRC well, the current source rock HTR is 60%, meaning that 60% of the original kerogen has been converted into hydrocarbons (Figures 16b and 17). As of approximately 4.1 million years ago, the HTR was 10%, indicating that hydrocarbon generation had increased significantly over that time period. As of approximately 0.46 million years ago, the HTR had increased to 50%, showing a more rapid increase in hydrocarbon generation closer to the present.

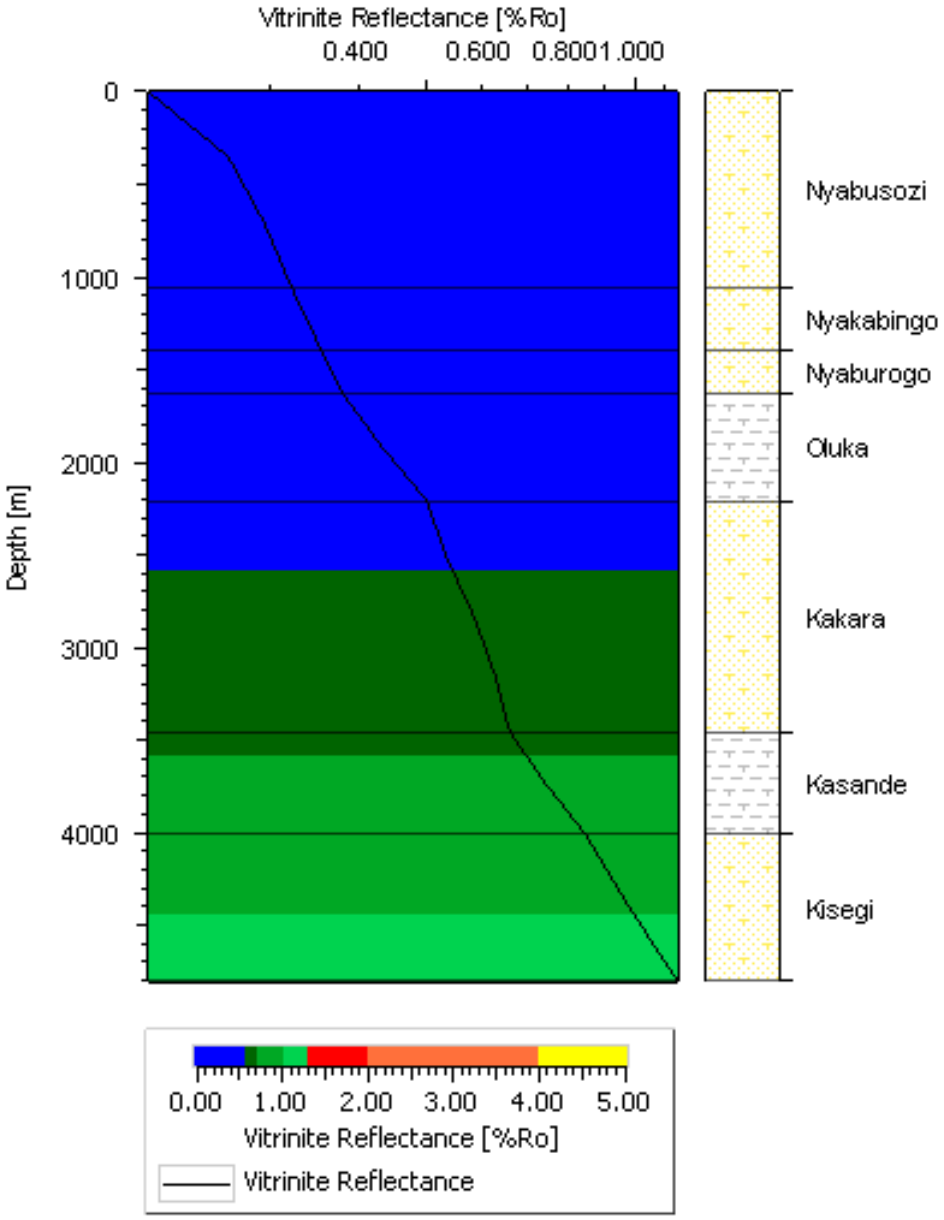

Figure 15. Modeled Vr plot for well X.

3.2.5. Petroleum System Elements

Petroleum system analysis reveals a complex interplay of elements within the Albert Rift basin. Key reservoirs identified include the Early Miocene Kisegi Formation and late Miocene Kakara Formation, and overburden formations such as the Mid-Pliocene-to-Recent Nyaburogo, Nyakabingo, and Nyabusozi formations. Source-rock analysis highlights the significant role of the Mid-Miocene Kasande Shale, which reached optimal thermal maturity during the late Pliocene, facilitating hydrocarbon generation and expulsion. The Late Miocene–Early Pliocene Oluka Formation acts as an effective seal, maintaining hydrocarbon entrapment conditions. Structural traps, formed during the Early Pliocene or earlier tectonic events, provide reservoir compartments favorable for hydrocarbon accumulation (Figure 18).

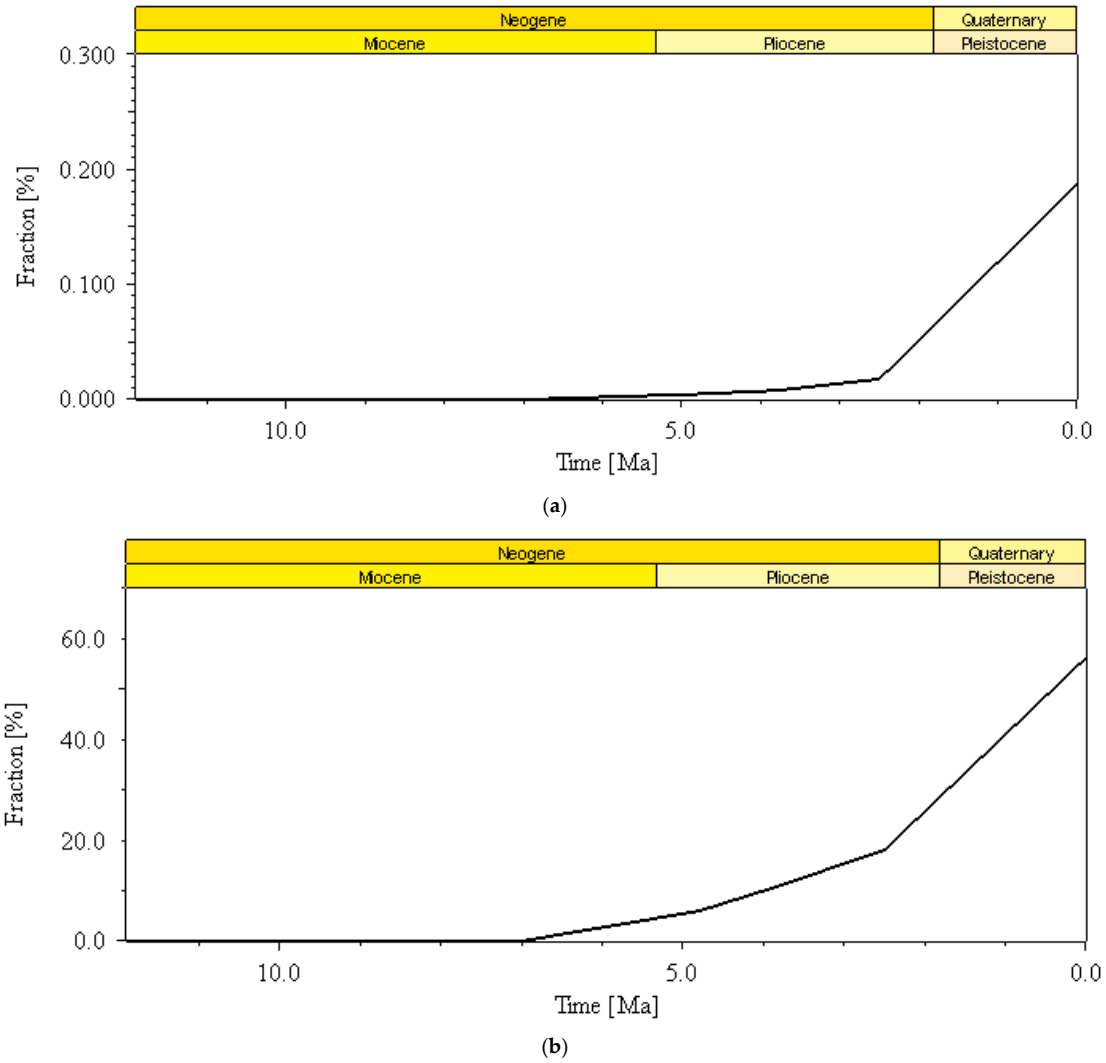

Figure 16. Hydrocarbon transformation plots for (**a**) well TRC and (**b**) well X.

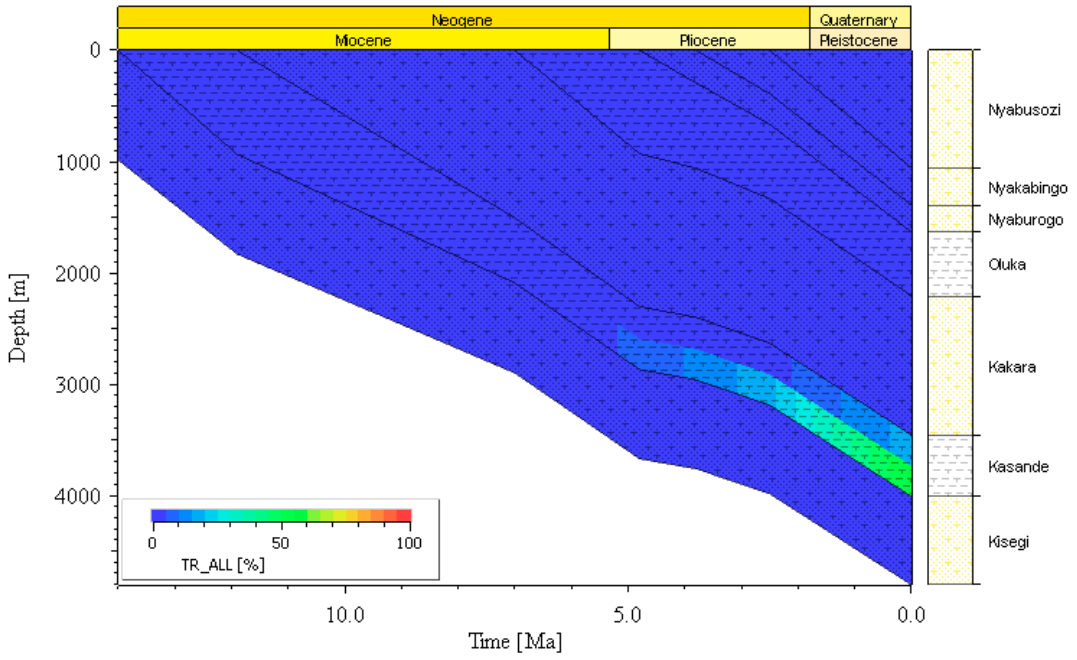

Figure 17. Source-rock hydrocarbon transformation during burial for well X.

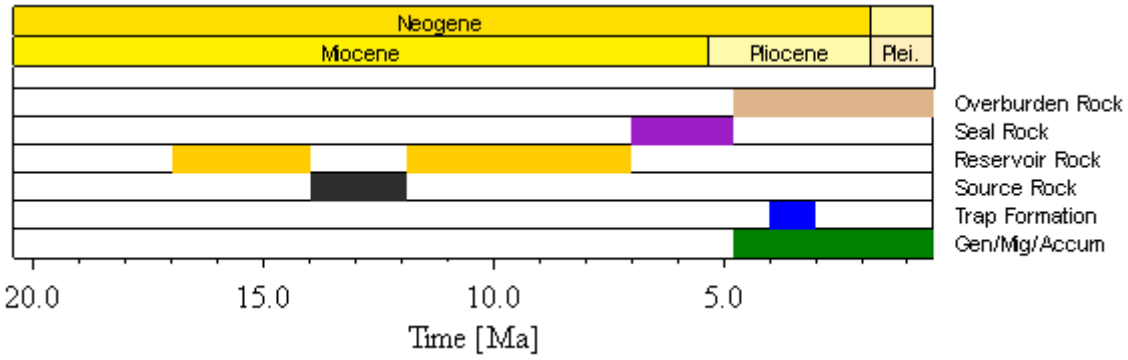

Figure 18. PetroMod-generated petroleum system events chart for the pseudo-well X.

4. Discussion

This section synthesizes the key findings from seismic interpretations, well-log analyses, geochemical characterizations, and Basin and Petroleum System Modeling (BPSM) to provide a comprehensive understanding of the tectono-stratigraphic evolution and hydrocarbon potential of the Albert Rift, Uganda. The results are interpreted in the context of basin development, structural deformation, depositional history, source-rock maturity, and hydrocarbon generation.

4.1. Tectonostratigraphic Evolution

The analysis of all the available data shows that the Albert Rift originated as a localized Semliki shallow basin during the Early Miocene, one dominated by fluvial sediment accumulation. It evolved into a lacustrine rift valley influenced by tectonic activity and climatic shifts, propagating north and south during the Upper Miocene and Lower Pliocene. The current rift-wide tectonostratigraphy shows temporal tectonics and sediment deposition stretching away from the central Semliki valley, supporting this progression. Similar patterns are observed in other EARS segments, including the Kenya Rift and Lakes Tanganyika, Malawi, and Rukwa, e.g., [40–43]. This initial localized evolution led to the deposition of the organic-rich source-rock facies, in confined niches controlled by the lacustrine extent, which are crucial for petroleum generation.

The southern Lake Albert Sub-basin has the most complete stratigraphy of the Albert Rift, with Early-Miocene-to-Recent sediments accessible from outcrops, and subsurface seismic and well data. This area hosts a sedimentary package of seven formations, each representing a particular depositional regime and time, forming four to five tectono-sedimentary phases [16,19,22,24,25,44]. This tectonic history matches the study's modeling results, showing a slightly non-uniform subsidence history with four to five phases. The first neotectonics phase represents slow subsidence from the Mid-Miocene to the beginning of the Upper Miocene. The second phase, from the Upper Miocene to the Early Pliocene, involves accelerated subsidence. These two phases probably coincide with the formation and evolution of a lacustrine rift recorded by the regional Lake Obweruka [16,24]. The third phase, from the Early to Late Pliocene, witnessed slower subsidence, and it is during this time that the separation of Lake Obweruka into Lakes Albert and Edward, around 2.5–3.0 Ma, is documented as having occurred [18,24,25]. Phase four involved accelerated subsidence from the Pleistocene to the present, coinciding with late regional rift shoulder uplift and tilting [24,25,45].

4.2. Source-Rock Hydrocarbon Potential and Depositional Environment

Geochemical and petrographic data from the NGJ, KWB, and TRC wells provide insights into the depositional environments and source-rock potential of the shales of the Albert Rift during the Miocene and Pliocene epochs. In the NGJ well, TOC values range

from 0.11% to 0.48%, indicating poor source-rock quality. HI values are in the range of 9–123 mgHC/g TOC, reflecting varying organic matter input, but exclusively gas-prone. The KWB well shows relatively higher organic richness, with TOC contents between 0.17% and 0.68% and HI values of 28–259 mgHC/g TOC, suggesting more oil-prone material compared to Well NGJ. In contrast, the TRC well exhibits significantly higher TOC values (0.56% to 7.99%, averaging 3.5%) and HI values of 89–502 mgHC/g TOC, with an average of 367 mgHC/g TOC, indicating good-to-excellent source-rock potential. The Kasande–Kakara–Oluka–Nyaburogo shale intervals in Well TRC, spanning the Mid-Miocene to Early Pliocene, are classified as good-to-very good source-rock facies. The lower section (Mid-Miocene) is predominantly oil-prone, while the upper section (Upper Miocene to Early Pliocene) is gas-prone. Organic microscopy of the samples as presented in the TRC well reports and other data show dominance of vitrinite and inertinite in the upper section e.g., [46], with the lower section containing strongly fluorescent algal kerogen, which explains the higher HI values.

The petrographic kerogen data (e.g., liptinite, amorphous organic matter, and vitrinite), total organic carbon (TOC), and hydrogen index (HI) trends observed in the TRC well suggest a strong environmental control over the organic matter type and hydrocarbon-generation potential.

Petrographic data from the TRC well indicate a predominance of Type I kerogens over Type III, with this dominance gradually decreasing from the lower to the upper sections of the succession. Kerogen type is a critical factor in determining the hydrocarbon potential of a source rock, as it dictates both the quantity and type of the hydrocarbons generated during thermal maturation. Kerogen is normally classified into four types: Type I (oil-prone), Type II (mixed oil and gas), Type III (gas-prone), and Type IV (inert). Type I kerogen, rich in hydrogen, is predominantly derived from lacustrine environments and generates mainly oil, especially at lower thermal maturities, while Type II, typically marine in origin, produces both oil and gas, with oil generation decreasing as thermal maturity increases, eventually shifting to gas at higher maturities. Type III kerogen, which is derived from terrestrial plant material, is gas-prone and predominantly produces natural gas, with gas generation intensifying as maturity exceeds the oil window. Type IV kerogen is largely inert and contributes little to hydrocarbon generation. The predominance of Type I kerogens suggests that the Albert Rift primarily represents an oil-prone system with limited gas generation. This interpretation is supported by the HI values presented in this paper.

Based on the high HI values and the predominance of oil-prone kerogen in the lower section of the well, it was hypothesized that these intervals were deposited in a nutrient-rich, eutrophic zone of an open lake, with minimal fluvial input, and that they have the potential for higher oil-to-gas generation ratios, compared to the upper sections with lower HI values. Such depositional settings, characterized by low terrigenous plant material influx, are often associated with high algal productivity, as seen in global analogs like the Green River Formation in the U.S. and the Eocene Mahakam Delta in Indonesia, where lacustrine to marginal lacustrine conditions are conducive to the deposition of high-quality, oil-prone source rocks [4,47]. The restricted fluvial influence in the lower TRC intervals likely limited land-plant detritus, resulting in a predominantly algal kerogen and contributing to the oil-prone character of the source rocks.

In contrast, the upper section of the TRC well, with its lower HI values and gas-prone signature, suggests an increased fluvial input and a transition to shallower lacustrine or deltaic environments. This shift is consistent with the sedimentological and geochemical trends observed in other lacustrine basins within rifts [48] and the Triassic Newark Super-group in the U.S., where deltas and shallow water environments tend to accumulate more

terrestrial organic matter, favoring gas generation due to the higher proportion of vitrinite and inertinite from land plants [49].

The KWB and NGJ wells, with their relatively low HI values and predominantly gas-prone character, appear to have been deposited in environments with significant terrestrial plant input, likely deltaic or marginal lacustrine settings with swampy vegetation-rich conditions. The well report review for the NGJ well further supports this depositional interpretation, given the evidence from palynomorph assemblages and lithological characteristics presented in this well report and our interpretations from the provided logs. These settings would be similar to the gas-prone source rocks observed in the deltaic sequences of the Niger Delta [50] and the Jurassic deltaic shales of the North Sea [51], where fluvial systems introduce abundant land plant detritus, resulting in the production of gas-prone kerogen.

The observed and measured parameters for the potential source-rock intervals are consistent with the current geological setting of the Albert Rift. The NGJ and KWB wells, drilled in more proximal zones, exhibit a higher potential for receiving terrestrial organic matter input. In contrast, the TRC well, located in a more distal zone of the rift, is characterized by predominantly lacustrine organic matter productivity and deposition.

4.3. Subsidence History

The modeled TRC well data indicate a slow subsidence rate during the initial stages of basin development, occurring between approximately 17 Ma and 8.0–7.0 Ma. While interpretations of this time period vary, it is broadly recognized as the early phase of rifting, characterized by low extensional rates and a correspondingly slow sedimentation rate, e.g., [24,25]. This aligns with global and regional analogs of early-stage rift basins, such as the different segments of the East African Rift System, in which tectonic stretching is gradual, leading to modest subsidence [48]. From 8.0–7.0 Ma to 4.0 Ma, the subsidence rate accelerates, reflecting increased tectonic activity and a more rapid sedimentation, which are typical of a mature rifting stage. This acceleration is often associated with more pronounced extensional faulting and greater accommodation space for sediment deposition, comparable to phases observed in other rift settings like the northwestern Red Sea in Egypt [52].

Between 4.0 Ma and 2.5 Ma, subsidence rates decrease, possibly linked to a reduction in rift extension and fault activity, suggesting a temporary tectonic quiescence. This period likely corresponds to reduced sediment influx as tectonic uplift and subsidence slowed.

From 2.5 Ma to the present, subsidence rates again accelerate, coinciding with major tectonic events, including the documented uplift of the Rwenzori Mountains and significant subsidence of the rift floor e.g., [2]. This phase is associated with intensified rift tectonics and increased sedimentation rates, driven by both tectonic uplift and enhanced erosion, as documented in the Late Pleistocene [2,22]. These tectonic and sedimentary dynamics have been suggested and documented by several authors e.g., [24,25,53,54].

4.4. Thermal Maturity, Hydrocarbon Generation and Expulsion

Measured Ro values in Well TRC increase from 0.24% at 620 m to 0.47% at 2330 m, indicating that most of the well section is too thermally immature for hydrocarbon generation. The top of the main oil generation window (Ro 0.5%) occurs at approximately 2500 m. Present-day geothermal gradient data suggest a higher maturity level than the measured values, possibly due to recent increases in heat flow and geothermal gradient near geothermal springs and shallow magma chambers [55–58]. The current hydrocarbon transformation ratio (HTR) of 0.2–0.3% for well TRC reflects a low level of hydrocarbon generation, with ongoing maturation. Pseudo-well X suggests that the source rock is in a peak oil window stage. The increase in Vr, from 0.66% Ro at the top to 0.84% Ro at the

base, indicates deeper burial and higher thermal maturity. The current HTR of 60% reflects an advanced hydrocarbon generation, with rapid increases in recent thermal burial. The Kasande shale, with advanced maturation and high HTR in the deeper sections, is a mature source rock with substantial hydrocarbon-generation potential. The progression of Vr and HTR over time indicates the presence of an effective hydrocarbon generation, which is likely to continue as it remains in the late stages of the oil window and approaches gas generation. This high HTR (60%) suggests a significant hydrocarbon expulsion, indicating the potential for migration into nearby reservoir rocks. Future exploration should focus on identifying and assessing potential reservoirs and migration pathways to predict potential hydrocarbon entrapment. Modeling results show that the Albert Rift is a young petroleum system, with hydrocarbon generation and expulsion starting in the Early-Mid-Pliocene in the depocenters. Some traps are still receiving hydrocarbons at present, suggesting potential for new accumulations in the rift. A clear understanding of the timing of petroleum generation and expulsion in relation to neo-tectonic evolution is crucial for identifying and assessing future hydrocarbon prospects. Seismic data from the Semliki and Lake Edward Basins indicate that the Albert Rift is highly faulted and likely compartmentalized, with a high concentration of both normal and reverse faults (e.g., Figure 8). Given the interbedded nature of shales and sandstones in the sedimentary section, shale smearing along faults may contribute to fault-sealing. Future studies should focus on determining the sealing or leaking capacities of these faults. In the Albert Rift, some fault systems act as conduits for fluid flow, whereas others act as barriers to fluid migration through mechanisms such as clay gouge development and fault zone alteration, which create low-permeability zones that effectively seal reservoirs [1]. Vertical hydrocarbon migration is particularly restricted where fine-grained formations, such as the Kasande and Oluka, are juxtaposed against the more permeable Kisegi and Kakara reservoir units. However, fault reactivation due to ongoing tectonic activity could compromise reservoir integrity by reopening previously sealed faults and creating new migration pathways, potentially leading to hydrocarbon leakage or redistribution outside of traps. This phenomenon is particularly evident in the Kasindi–Bantu Fault Zone in the Lake Edward Basin, where fault reactivation may influence both fluid migration and hydrocarbon accumulation in apron fans and deltaic systems, as evidenced by a string of oil seeps. Oil seeps along faults are a common feature in the Albert Rift, underscoring the potential negative impact of faulting on reservoir integrity. Previous studies (e.g., [2,15,22,24,25]) suggest that before the Pliocene–Pleistocene boundary, the Albert Rift functioned as a single fluvial–lacustrine system hosting a unified regional petroleum system. The uplift of the Rwenzori Massif subsequently compartmentalized the rift into two main basins, north and south of the massif. This event, along with continued tectonic activity, likely played a crucial role in breaching earlier traps and forming new ones. Further investigations will be necessary to refine this understanding as more subsurface data become available.

5. Conclusions

This study presents a comprehensive analysis of the geological evolution and petroleum systems of the Albert Rift, Uganda, integrating seismic, well, and outcrop data with data from the literature, and using Basin and Petroleum System Modeling (BPSM) to provide a detailed tectonostratigraphic framework for the rift.

Key findings include the following:

1. The identification and characterization of depositional units and structural features, forming the basis for a refined tectonostratigraphic framework outlining the temporal and spatial evolution of the Neogene rift basin.

2. The significant influence of rift propagation on basin architecture and stratigraphy, which governs the distribution and quality of source, reservoir, and seal rocks, with major implications for petroleum systems. Four distinct phases of subsidence, with well-defined timing, are documented in the TRC model, providing an important milestone for reconciling previous tectono-sedimentary models.
3. Geochemical analysis indicates that Mid-Miocene sediments were deposited in favorable lacustrine environments conducive to source-rock formation. BPSM results demonstrate the hydrocarbon generation and expulsion processes, with thermal maturity increasing northwestward toward the depocenters. These findings suggest that the Mid-Miocene lacustrine source rocks in deeper basin areas began generating and expelling hydrocarbons from the Middle to Late Pliocene, while those in shallower regions have only recently entered the oil window. The study further shows that sediments in the northwest reached the oil window earlier than those in the southeast, which would be consistent with regional structural dips.

This study lays a strong foundation for future exploration in the Albert Rift, offering valuable insights into the timing and mechanisms of hydrocarbon generation and expulsion. The integration of stratigraphic and petroleum system analyses provides a comprehensive understanding of the controlling factors, which are applicable to similar rift basins worldwide. Notably, the evidence suggests that younger source rocks, post-dating the Mid-Miocene, are unlikely to have generated or expelled hydrocarbons. As such, the existing stratigraphic models that suggest a Mid-Miocene lacustrine rift are likely more accurate than those proposing a younger rift initiation. This investigation further suggests that future exploration efforts should focus on the Southern Lake Albert sector, where petroleum generation and expulsion potential remain highly promising, despite the lack of commercial discoveries to date. The study underscores the effectiveness of BPSM in resolving stratigraphic uncertainties in frontier basins with limited data, demonstrating its role in harmonizing divergent geological interpretations. It further supports models advocating for an Early Miocene basin initiation, one followed by Mid-Miocene rifting and lacustrine deposition, and contrasts with Late Miocene initiation models, which do not align with the calibrated results. This work advances the geological understanding of the Albert Rift and exemplifies the value of integrated basin analysis. Future research should focus on refining stratigraphic correlations and investigating deeper, untested strata to further assess hydrocarbon potential.

Author Contributions: Conceptualization, L.T. and K.L.; methodology, L.T. and K.L.; software, S.W. and H.A.R.H.; validation, K.L., K.J. and T.S.; formal analysis, L.T.; investigation, L.T.; resources, K.J.; data curation, L.T., M.S. and S.W.; writing—original draft preparation, L.T.; writing—review and editing, K.L.; visualization, L.T.; supervision, K.L.; project administration, K.L.; funding acquisition, K.L. All authors have read and agreed to the published version of the manuscript.

Funding: This work was supported by the Major Research Project on the Tethys Geodynamic System of the National Natural Science Foundation of China (No. 92055204).

Institutional Review Board Statement: Not applicable.

Informed Consent Statement: Not applicable.

Data Availability Statement: Restrictions apply to the availability of these data. Data were obtained from the Government of Uganda and are available with permission.

Acknowledgments: We acknowledge the Government of Uganda and Chinese Government Scholarship Council for providing data and financial support, respectively.

Conflicts of Interest: The authors declare no conflicts of interest.

References

1. Abeinomugisha, D.; Njabire, N. Transfer Zones and Hydrocarbon Accumulation in the Albertine Graben of the East African Rift System. *AAPG Annu. Conv. Exhib.* **2012**, *10401*, 8.
2. Hinderer, M.; Schneider, S.; Stutenbecker, L. Unravelling the evolution of a continental rift by a multi-proxy provenance study (Albertine Rift, Uganda). *Int. J. Earth Sci.* **2024**, *113*, 1317–1336. [CrossRef]
3. Talbot, M.R. The origins of lacustrine oil source rocks: Evidence from the lakes of tropical Africa. *Geol. Soc. Lond. Spec. Publ.* **1988**, *40*, 29–43. [CrossRef]
4. Katz, B.J. Controls on distribution of lacustrine source rocks through time and space. In *Lacustrine Basin Exploration: Case Studies and Modern Analogs*; Katz, B.J., Ed.; AAPG: Tulsa, OK, USA, 1990; Volume 50, pp. 61–76.
5. Rosendahl, B.R.; Kilembe, E.; Kaczmarick, K. Comparison of the Tanganyika, Malawi, Rukwa and Turkana Rift zones from analyses of seismic reflection data. *Tectonophysics* **1992**, *213*, 235–256. [CrossRef]
6. Scholz, C.A. Deltas of the Lake Malawi rift, East Africa: Seismic expression and exploration implications. *AAPG Bull.* **1995**, *79*, 1679–1697.
7. Soreghan, M.J.; Cohen, A.S. Textural and compositional variability across littoral segments of Lake Tanganyika: The effect of asymmetric basin structure on sedimentation in large rift lakes. *AAPG Bull.* **1996**, *80*, 382–409.
8. Demaison, G.J.; Moore, G.T. Anoxic environments and oil source bed genesis. *Org. Geochem.* **1980**, *2*, 9–31. [CrossRef]
9. Karp, T.; Scholz, C.A.; McGlue, M.M. Structure and Stratigraphy of the Lake Albert Rift, East Africa Observations from Seismic Reflection and Gravity Data. In *Lacustrine Sandstone Reservoirs and Hydrocarbon Systems*; AAPG: Tulsa, OK, USA, 2012. [CrossRef]
10. Morley, C.K.; Nelson, R.A.; Patton, T.L.; Munn, S.G. Transfer zones in the East African rift system and their relevance to hydrocarbon exploration in rifts. *AAPG Bull.* **1990**, *74*, 1234–1253. [CrossRef]
11. Macgregor, D. History of the development of the East African Rift System: A series of interpreted maps through time. *J. Afr. Earth Sci.* **2015**, *101*, 232–252. [CrossRef]
12. Abrahao, D.; Warme, J.E. Lacustrine and associated deposits in a rifted continental margin: Lower Cretaceous Lagoa Feia Formation, Campos Basin, offshore Brazil. In *Lacustrine Basin Exploration: Case Studies and Modern Analogs*; Katz, B.J., Ed.; AAPG: Tulsa, OK, USA, 1990; Volume 50, pp. 287–305.
13. McHargue, T.R. Stratigraphic development of proto-South Atlantic rifting in Cabinda, Angola: A petroliferous lake basin. In *Lacustrine Basin Exploration: Case Studies and Modern Analogs*; Katz, B.J., Ed.; AAPG: Tulsa, OK, USA, 1990; Volume 50, pp. 307–326.
14. Pickford, M. *Field Report—Western Rift*; Unpublished Field Report; Collège de France: Paris, France, 2011; pp. 1–30.
15. Pickford, M.; Senut, B. *Western Rift Valley*; Unpublished Field Report; Collège de France: Paris, France, 2012; pp. 1–61.
16. Lukaye, J.; Worsley, D.; Kiconco, L.; Nabbanja, P.; Abeinomugisha, D.; Amusugut, C.; Njabire, N.; Nuwagaba, R.; Mugisha, F.; Ddungu, T.; et al. Developing a coherent stratigraphic scheme of the Albertine Graben-East, Africa. *Glob. J. Earth Sci. Eng.* **2016**, *6*, 264–294. [CrossRef]
17. Lukaye, J.; Etano, G.; Abbott, G. Molecular organic geochemistry of crude oils from the Albertine Graben, Uganda: Possible implications on the expulsion of the oils from the source rocks. *Glob. J. Earth Sci. Eng.* **2017**, *7*, 181–193. [CrossRef]
18. Pickford, M.; Senut, B.; Hadoto, D. *Geology and Palaeobiology of the Albertine Rift Valley, Uganda-Zaire*; CIFEG: Orléans, France, 1993; Volume 1, p. 189.
19. Bauer, F.U.; Glasmacher, U.A.; Ring, U.; Grobe, R.W.; Mambo, V.S.; Starz, M. Long-term cooling history of the Albertine Rift: New evidence from the western rift shoulder, DR Congo. *Int. J. Earth Sci.* **2016**, *105*, 1707–1728. [CrossRef]
20. Jess, S.; Koehn, D.; Fox, M.; Enkelmann, E.; Sachau, T.; Aanyu, K. Paleogene initiation of the Western branch of the east African Rift: The uplift history of the Rwenzori Mountains, Western Uganda. Earth Planet. *Sci. Lett.* **2020**, *552*, 116593. [CrossRef]
21. Michon, L.; Famin, V.; Quidelleur, X. Evolution of the East African Rift System from trap-scale to plate-scale rifting. *Earth Sci. Rev.* **2022**, *231*, 104089. [CrossRef]
22. Schneider, S.; Hornung, J.; Hinderer, M. Evolution of the western East African Rift System reflected in provenance changes of Miocene to Pleistocene synrift sediments (Albertine Rift, Uganda). *Sediment. Geol.* **2016**, *343*, 190–205. [CrossRef]
23. Lukaye, J.M. Biostratigraphy and palynofacies of four exploration wells from the Albertine Graben, Uganda. *Am. Assoc. Pet. Geol. Search Discov. Artic.* **2009**, 50169. Available online: https://www.searchanddiscovery.com/documents/2009/50169lukaye/ndx_lukaye.pdf (accessed on 1 March 2025).
24. Roller, S.; Hornung, J.; Hinderer, M.; Ssemmanda, I. Middle Miocene to Pleistocene sedimentary record of rift evolution in the southern Albert Rift (Uganda). *Int. J. Earth Sci.* **2010**, *99*, 1643–1661. [CrossRef]
25. Simon, B.; Guillocheau, F.; Robin, C.; Dauteuil, O.; Nalpas, T.; Pickford, M.; Bez, M. Deformation and sedimentary evolution of the Lake Albert rift (Uganda, East African Rift System). *Mar. Pet. Geol.* **2017**, *86*, 17–37. [CrossRef]
26. Lukaye, J.; Okello, M. Geochemical Characterization and Correlation of Crude Oils and Potential Source Rocks from the Semliki, Southern Lake Albert and Kaisotonya basins in the Albertine Graben, Uganda. In Proceedings of the International Conference and Exhibition, Melbourne, Australia, 13–16 September 2015; p. 557. [CrossRef]

27. Klemme, H.D.; Ulmishek, G.F. Effective petroleum source rocks of the world: Stratigraphic distribution and controlling depositional factors. *AAPG Bull.* **1991**, *75*, 1809–1851.
28. Tissot, B.P.; Pelet, R.; Ungerer, P. Thermal History of Sedimentary Basins, Maturation Indices, and Kinetics of Oil and Gas Generation. *AAPG Bull.* **1987**, *71*, 1445–1466. [CrossRef]
29. Welte, D.H.; Yalçin, M.N. Basin Modelling-A New Comprehensive Method in Petroleum Geology. *Org. Geochem.* **1988**, *13*, 141–151. [CrossRef]
30. Ungerer, P.; Burrus, J.; Doligez, B.; Chenet, P.Y.; Bessis, F. Basin Evaluation by Integrated Two-Dimensional Modeling of Heat Transfer, Fluid Flow, Hydrocarbon Generation, and Migration. *AAPG* **1990**, *74*, 309–335. [CrossRef]
31. Higley, D.K.; Michael, L.; Laura, N.R.R.; Mitchell, E.H. *Petroleum System Modeling Capacities for Use in Oil and Gas Resource Assessments*; U.S. Geological Survey: Liston, VA, USA, 2006. [CrossRef]
32. Hantschel, T.; Kauerauf, A.I. *Fundamentals of Basin and Petroleum Systems Modeling*; Springer Science & Business Media: Berlin/Heidelberg, Germany, 2009; p. 476. [CrossRef]
33. Peters, K.E.; Schenk, O.; Hosford, S.A.; Wygrala, B.; Hantschel, T. Basin and Petroleum System Modeling. In *Handbook of Petroleum Technology*; Springer: Berlin/Heidelberg, Germany, 2017; pp. 381–417. [CrossRef]
34. Baur, F.; Scheirer, A.H.; Peters, K.E. Past, present, and future of basin and petroleum system modeling. *AAPG Bull.* **2018**, *102*, 549–561. [CrossRef]
35. Tugume, F.A.; Nyblade, A.A. The depth distribution of seismicity at the northern end of the Rwenzori mountains: Implications for heat flow in the western branch of the East African Rift System in Uganda. *S. Afr. J. Geol.* **2009**, *112*, 261–276. [CrossRef]
36. Sweeney, J.J.; Burnham, A.K. Evaluation of a simple model of vitrinite reflectance based on chemical kinetics. *AAPG Bull.* **1990**, *74*, 1559–1570. [CrossRef]
37. Frakes, L.A. *Climates Throughout Geological Time*; Elsevier: Amsterdam, The Netherlands, 1979; pp. 1–310.
38. Hardenbol, J.; Thierry, J.; Farley, M.; Thierry, J.; De Graciansky, P.C.; Vail, P.R. *Mesozoic and Cenozoic Stratigraphy of European Basins*; SEPM Society for Sedimentary Geology: Tulsa, OK, USA, 1998; Volume 60. [CrossRef]
39. Dembicki, H. *Practical Petroleum Geochemistry for Exploration and Production*; Elsevier: Amsterdam, The Netherlands, 2017; pp. 1–331.
40. Mechie, J.; Keller, G.R.; Prodehl, C.; Khan, M.A.; Gaciri, S.J. A model for the structure, composition and evolution of the Kenya rift. *Tectonophysics* **1997**, *278*, 95–119. [CrossRef]
41. Ebinger, C.J.; Casey, M. Continental breakup in magmatic provinces: An Ethiopian example. *Geol. J.* **2001**, *29*, 527–530. [CrossRef]
42. Hofstetter, R.; Beyth, M. The Afar Depression: Interpretation of the 1960–2000 earthquakes. *Geophys. J. Int.* **2003**, *155*, 715–732. [CrossRef]
43. Shaban, S.N.; Scholz, C.A.; Muirhead, J.D.; Wood, D.A. The stratigraphic evolution of the Lake Tanganyika Rift, East Africa: Facies distributions and paleo-environmental implications. *Palaeogeogr. Palaeoclimatol. Palaeoecol.* **2021**, *575*, 110474. [CrossRef]
44. Bauer, F.U.; Glasmacher, U.A.; Ring, U.; Schumann, A.; Nagudi, B. Thermal and exhumation history of the central Rwenzori Mountains, Western rift of the east African rift system, Uganda. *Int. J. Earth Sci.* **2010**, *99*, 1575–1597. [CrossRef]
45. Nicholas, C.J.; Newth, I.R.; Abeinomugisha, D.; Tumushabe, W.M.; Twinomujuni, L. Geology and stratigraphy of the south-eastern Lake Edward basin (Petroleum Exploration Area 4B), Albertine Rift Valley, Uganda. *J. Maps.* **2016**, *12*, 237–248. [CrossRef]
46. Mutebi, S.; Sen, S.; Sserubiri, T.; Rudra, A.; Ganguli, S.S.; Radwan, A.E. Geological characterization of the Miocene–Pliocene succession in the Semliki Basin, Uganda: Implications for hydrocarbon exploration and drilling in the East African Rift System. *Nat. Resour. Res.* **2021**, *30*, 4329–4354. [CrossRef]
47. Tissot, B.P.; Welte, D.H. *Petroleum Formation and Occurrence*; Springer Science & Business Media: Berlin/Heidelberg, Germany, 2013; pp. 1–679.
48. Morley, C.K. Tectonic settings of continental extensional provinces and their impact on sedimentation and hydrocarbon prospectivity. In *Sedimentation in Continental Rifts*; Renaut, R.W., Ashley., G.M., Eds.; Society for Sedimentary Geology: Broken Arrow, OK, USA, 2002. [CrossRef]
49. Peters, K.E.; Cassa, M.R. Applied Source Rock Geochemistry. In *The Petroleum System—From Source to Trap*; AAPG: Tulsa, OK, USA, 1994; Volume 60, pp. 93–120.
50. Doust, H.; Omatsola, E. Niger Delta. In *Divergent/Passive Margin Basins*; Edwards, J.D., Santogrossi, P.A., Eds.; AAPG: Tulsa, OK, USA, 1990; Volume 48, pp. 239–248.
51. Cornford, C. Source Rocks and Hydrocarbons of the North Sea. In *Petroleum Geology of the North Sea*; Glennie, K.W., Ed.; Blackwell Publishing: Oxford, UK, 1998; pp. 376–462.
52. McClay, K.; Khalil, S.M.; Bosworth, W.; Gussinye, M.P. *Tectono-Stratigraphic Evolution of the Northwestern Red Sea, Egypt–A Review*; Rifting and Sediments in the Red Sea and Arabian Gulf Regions; CRC Press: Boca Raton, FL, USA, 2024; pp. 9–36.
53. Van Damme, D.; Pickford, M. The late Cenozoic ampullariidae (mollusca, gastropoda) of the Albertine rift valley (Uganda-Zaire). *Hydrobiologia* **1995**, *316*, 1–32. [CrossRef]

54. Van Damme, D.; Pickford, M. The late Cenozoic Thiaridae (Mollusca, Gastropoda, Cerithioidea) of the Albertine rift valley (Uganda-Congo) and their bearing on the origin and evolution of the Tanganyikan thalassoid malacofauna. *Hydrobiologia* **2003**, *498*, 1–83. [CrossRef]
55. Kato, V. Geothermal exploration in Uganda—Status report. In *SDG Short Course II on Exploration and Development of Geothermal Resources, Organized by UNU-GTP, GDC and KenGen, at Lake Bogoria and Lake Naivasha, Kenya*; 2016; pp. 1–24. Available online: https://www.academia.edu/85154315/Geothermal_Exploration_in_Uganda (accessed on 1 March 2025).
56. EAGER. *Structural Geology at Panyimur and Buranga*; East Africa Geothermal Energy Facility, Report U-23-D02; EAGER, Ministry of Mineral Development: Kampala, Uganda, 2017; 11p.
57. Hinz, N.; Cumming, B.; Sussman, D. Exploration of fault-related deep-circulation geothermal resources in the western branch of the East African Rift System: Examples from Uganda and Tanzania. In Proceedings of the 7th African Rift Geothermal Conference, Kigali, Rwanda, 31 October–2 November 2018; pp. 1–16.
58. Kahwa, E. Geothermal Exploration in Uganda—Status Report . In *SDG Short Course II on Exploration and Development of Geothermal Resources, Organized by UNU-GTP, GDC and KenGen, at Lake Bogoria and Lake Naivasha, Kenya*; 2021; pp. 1–11. Available online: https://www.grocentre.is/static/files/GTP/ShortCourses/SC-29/0706geothermaldevelopmentugandaek2101.pdf (accessed on 1 March 2025).